

Ana Sofia Soares Mendes

BSc Cellular and Molecular Biology

**Carbon Monoxide Releasing Molecules - towards a novel
antimicrobial therapeutic drug**

Dissertation to obtain the Master Degree in Biochemistry for Health

Supervisor: Lúgia Saraiva, Principal Investigator, ITQB-UNL

Co-supervisor: Joana Marques, Post-doc, ITQB-UNL

Jury members:

President: Pedro Matias, PhD

Opponent: Miguel Teixeira, PhD

Vowel: Lúgia Saraiva, PhD

Instituto de Tecnologia Química e Biológica António Xavier – UNL

September 2018



Top row, from left to right: Patrícia Ferreira, Cátia Família, Joana Marques, Lúgia Saraiva, Marco Videira and Ana Sofia Mendes.

Bottom row, from left to right: Cláudia Freitas, Sandra Carvalho and Líliana Silva.

November 11th, 2017.

Carbon Monoxide Releasing Molecules - towards a novel antimicrobial therapeutic drug

Copyright © Ana Sofia Soares Mendes, ITQB and UNL

The Instituto de Tecnologia Química e Biológica António Xavier and the Universidade Nova de Lisboa have the right, perpetual and without geographical limits, to file and publish this dissertation through printed copies reproduced on paper or on digital form, or by any other means known or that may be invented, and to disseminate through scientific repositories and admit its copying and distribution for non-commercial, educational or research purposes, as long as credit is given to the author and editor.

Acknowledgments

I would like to express my sincere gratitude to the people without whom this dissertation would have not been possible:

To Doctor Lígia Saraiva, for receiving me in her laboratory and accepting to be my supervisor. To supporting and believing in me, and for the endless patience in helping me with my thesis. Thank you for all the talks and advices and for all the confidence placed in me.

To Joana Marques, for all the advices and encouragement that you gave me. Thank you for being honest, and for criticizing and cheering me when I needed the most. Thank you for your friendship and for all the talks and laughs that we had. I also want to thank you for all the knowledge that you have passed to me.

To professor Carlos Romão, for the collaboration on this work and for enlightening me on several conversations about CORMs.

To Cláudia Freitas, for being a friend throughout this last year, and for listening to me and helping me when I needed. Thank you for all the talks, advices and craziness! To Sandra Carvalho, for always knowing what to say and for teaching me new things all the time! To Liliana Silva, for being funny and for being always willing to aid me! To Marco Videira, for all the whining and playfulness! To Cátia Família, for all the frontality and honest advices! The Lab life would have not be as fun without you guys!

To my Mom and Dad who always supported me and believed in my abilities, and for all the years of love. For all the strength that you gave me and for always making sure that my life was in every aspect complete! To my family who was always there for me and that always held me when I needed!

To my friends who gave me a mental escape and made sure I was happy no matter what. Thank you for being by my side in every moment! To Miki, Lucky and Kiara, who were always there whenever I got home and needed to cuddle!

To Mário del Santoro, for the constant love and support, and for never letting me beat myself up in any moment. Thank you for making me feel happy and loved every day!

This dissertation is dedicated to my parents

Abstract

Carbon monoxide releasing molecules (CORMs) are carbonyl organometallic complexes that liberate controlled amounts of carbon monoxide, which is a signalling and cytoprotective molecule important in human physiology and pathophysiology. Several studies in animals have shown that CORMs are beneficial in the treatment of cardiovascular diseases, inflammation and organ protection. Additionally, CORMs present antimicrobial properties.

In this master thesis, 18 CORMs were studied, which when organised according to the metal centre form 3 families of complexes, together with the 8 organic ligands used for CORM-coordination and the respective solvents. Firstly, the antimicrobial action against pathogens was determined. For the more active CORMs, the interaction with bacterial cells and cytotoxicity to mammalian cells was also investigated.

Data showed that some of these compounds are more active than CORM-3, the prototype of CORMs, against Gram-negative bacteria. Moreover, two CORMs JM46 and JM47 were observed to kill efficiently Gram-positive bacteria with minimum inhibitory concentrations lower than 2 $\mu\text{g/ml}$. For these more potent CORMs it was determined, by myoglobin assays and fluorescence microscopy, the release of CO *in vitro* and inside bacterial cells. Importantly, CORMs JM46 and JM47 caused alteration on bacterial cell wall, as observed by fluorescence microscopy, that might explain their antimicrobial activity.

Altogether, new CORMs were investigated and progress towards obtaining a more efficient bactericide based on CO releasing molecules was made.

Keywords: Carbon Monoxide (CO); CORMs; Bacterial Pathogens; Antimicrobials.

Resumo

Moléculas libertadoras de monóxido de carbono (CORMs) são complexos organometálicos com ligandos carbonilo que libertam quantidades controladas de monóxido de carbono, que é uma molécula sinalizadora e citoprotetora importante na fisiologia e patofisiologia humana. Vários estudos em animais demonstraram que os CORMs são benéficos no tratamento de doenças cardiovasculares, processos inflamatórios e na proteção de órgãos. Adicionalmente, os CORMs apresentam propriedades antimicrobianas.

Nesta dissertação de mestrado, foram estudados 18 CORMs, que quando organizados de acordo com o centro metálico formam 3 famílias, juntamente com os 8 ligandos orgânicos usados nos complexos e os respectivos solventes. Primeiramente, foi determinada a ação antimicrobiana contra diferentes agentes patogénicos. Para os CORMs mais ativos, também foi investigada a interação com células bacterianas e a toxicidade em células animais.

Os resultados demonstraram que alguns destes compostos são mais ativos contra bactérias Gram-negativas que o CORM-3, um protótipo dos CORMs. Adicionalmente, observou-se que os dois CORMs JM46 e JM47 matam eficazmente bactérias Gram-positivas, com concentração mínima de inibição de crescimento inferior a 2 µg/ml. Para estes CORMs mais potentes, foi determinado o perfil de libertação de CO *in vitro* e dentro de células bacterianas através de ensaios com mioglobina e microscopia de fluorescência, respectivamente. É de realçar que os CORMs JM46 e JM47 causam alterações na parede celular bacteriana, como observado por microscopia de fluorescência, o que pode explicar a sua actividade antimicrobiana.

Assim, foram investigados novos CORMs e feitos progressos na obtenção de um bactericida mais eficiente com base em moléculas libertadoras de monóxido de carbono.

Palavras-chave: Monóxido de Carbono (CO); CORMs; Patogénios bacterianos; Antimicrobianos.

Table of Contents

Acknowledgments	iii
Abstract	v
Resumo	vii
List of Figures	xi
List of Tables	xv
List of Abbreviations	xvii
1 Introduction	1
1.1 Carbon Monoxide	1
1.2 Carbon monoxide therapies	3
1.3 Bacteria	4
1.3.1 <i>Escherichia coli</i>	4
1.3.2 <i>Salmonella enterica</i>	5
1.3.3 <i>Staphylococcus aureus</i>	6
1.4 Antibiotic Resistance	7
1.5 Carbon Monoxide Releasing Molecules (CORMs)	9
1.5.1 <i>Carbon monoxide releasing molecules as bactericides</i>	12
1.6 Aim of this work	16
2 Materials and Methods	17
2.1 CORMs, ligands and solvents	18
2.2 Bacterial strains and growth conditions	19
2.3 Minimum Inhibitory Concentration assay	20
2.4 Bacterial cell membrane permeability assay	21
2.5 Detection of CO release from CORMs	22
2.5.1 <i>Myoglobin assay</i>	22
2.5.2 <i>Intracellular detection of CO released from CORMs</i>	23
2.6 Animal cell culture and toxicity assay	24
3 Results	27
3.1 CORMs and ligands	27
3.2 Determination of the Minimum Inhibitory Concentrations	28
3.3 Bacterial growth with CORMs	30
3.4 Bacterial cell membrane permeability	36
3.5 Myoglobin assay	39
3.6 Intracellular detection of CO released from CORMs	42
3.7 Animal cell toxicity assays	45
4 Discussion	49

5	Conclusions and future perspectives.....	57
	Bibliography.....	59
	Supplementary material.....	65

List of Figures

Figure 1.1 Carbon monoxide poisoning symptoms. Reprinted from Romão <i>et al.</i> (2012).	1
Figure 1.2 Catalytic mechanism of haem oxygenase. Haem is degraded by haem oxygenase (HO), originating biliverdin, free iron (Fe^{2+}) and carbon monoxide (CO). Biliverdin is then converted to bilirubin by biliverdin reductase (BVR).	2
Figure 1.3 Schematic representation of the effects of CO on different areas of the organism. Reprinted from Nakahira <i>et al.</i> (2015).	3
Figure 1.4 Scanning electron microscope photography of <i>Escherichia coli</i> . Reprinted from scharfphotography.com.	4
Figure 1.5 Scanning electron microscope photography of <i>Salmonella enterica</i> . Reprinted from scharfphotography.com.	5
Figure 1.6 Scanning electron microscope photography of <i>Staphylococcus aureus</i> . Reprinted from scharfphotography.com.	6
Figure 1.7 Carbon monoxide administration methods and its advantages. Reprinted from Romão <i>et al.</i> (2012).	10
Figure 1.8 Schematic representation of the construction of CORMs with pharmacological purposes. Reprinted from Romão <i>et al.</i> (2012).	11
Figure 1.9 Organometallic molecule on the top right corner, and different coordination ligands at the bottom. The metal-coordinated atom is highlighted in grey. Adapted from Simpson <i>et al.</i> (2015).	15
Figure 2.1 Cell membrane permeability assay. SYTO TM 9 (green circle) can enter all cells (live and dead) whereas propidium iodide (red hexagon) can only enter permeable cells (dead).	21
Figure 2.2 Absorbance spectra of Reduced myoglobin (Mb) and carbonmonoxy-myoglobin (Mb-CO).	23
Figure 2.3 Carbonylation reaction of COP-1. Adapted from Michel <i>et al.</i> (2012).	23
Figure 3.1 Growth curve of <i>E. coli</i> over 24 hours after treatment with 35 μM of JM46, JM20, JM47, JM20Re, clotrimazole or 1 % DMSO, as control.	31
Figure 3.2 Growth curve of <i>S. enterica</i> over 24 hours after treatment with 35 μM of JM46, JM20, JM47, JM20Re, clotrimazole or 1 % DMSO, as control.	32
Figure 3.3 Growth curve of <i>S. aureus</i> over 24 hours after treatment with 10 μM of JM46, JM20, JM47, JM20Re, clotrimazole or 1 % DMSO, as control.	32
Figure 3.4 <i>Escherichia coli</i> growth inhibition 2 and 4 hours after exposure to 250 μM of: (A) CORM-3, JM94, JM106, JM14 and JM16; and (B) ctz – clotrimazole; bpy – bipyridyl; phen – phenanthroline.	34
Figure 3.5 <i>Salmonella enterica</i> growth inhibition 2 and 4 hours after exposure to 250 μM of:	35

- (A) CORM-3, JM94, JM106, JM14 and JM16; and (B) ctz – clotrimazole; bpy – bipyridyl; phen – phenanthroline.
- Figure 3.6** *Staphylococcus aureus* growth inhibition 2 and 4 hours after exposure to 250 μM of: (A) CORM-3, JM94, JM106, JM14 and JM16; and (B) ctz – clotrimazole; bpy – bipyridyl; phen – phenanthroline. 35
- Figure 3.7** *E. coli* cell membrane permeability upon treatment with CORMs. Microscope images of the effect of JM46 and JM47 after 2 and 24 hours of incubation, evaluated by the Live/Dead viability staining method. Live and healthy bacteria with intact membrane are stained green (SYTO9), and dead bacteria or unhealthy with damaged membranes are stained yellow-red (propidium iodide). 37
- Figure 3.8** *S. enterica* cell membrane permeability upon treatment with CORMs. Microscope images of the effect of JM46 and JM47 after 2 and 24 hours of incubation, evaluated by the Live/Dead viability staining method. Live and healthy bacteria with intact membrane are stained green (SYTO9), and dead bacteria or unhealthy with damaged membranes are stained yellow-red (propidium iodide). 38
- Figure 3.9** *S. aureus* cell membrane permeability upon treatment with CORMs. Microscope images of the effect of JM46 and JM47 after 2 and 24 hours of incubation, evaluated by the Live/Dead viability staining method. Live and healthy bacteria with intact membrane are stained green (SYTO9), and dead bacteria or unhealthy with damaged membranes are stained yellow-red (propidium iodide). 39
- Figure 3.10** Absorbance spectra of myoglobin (Mb) represented by the dashed black line, and carbonmonoxy-myoglobin (Mb-CO) represented by the full grey line. 40
- Figure 3.11** Absorbance spectra of myoglobin (Mb) in the presence of JM46, JM47, JM20 and JM20R for 120 minutes. Spectra were obtained at 0 minutes (burgundy), 30 minutes (green), 60 minutes (purple), 90 minutes (blue) and 120 minutes (orange). 41
- Figure 3.12** Detection of CO release intracellularly utilizing a fluorescent probe, COP-1. Microscope images of three organisms: *E. coli* (first row), *S. enterica* (second row) and *S. aureus* (third row), after exposure to two CORMs: JM46 (left column) and JM47 (right column). Each column presents a microscopy image (Brightfield) and the correspondent fluorescent image (FITC). 42
- Figure 3.13** Detection of CO release intracellularly utilizing a fluorescent probe, COP-1. Microscope images of three organisms: *E. coli* (first row), *S. enterica* (second row) and *S. aureus* (third row), after exposure to DMSO (1 %). For each organism there is a microscopy image (Brightfield) and the correspondent fluorescent image (FITC). 43
- Figure 3.14** Cytotoxicity of CORMs and ligands was evaluated in LLC-PK1, using (A) JM46, (B) JM47, (C) JM60, (D) JM97, (E) JM107, (F) JM108, (G) JM109 and (H) clotrimazole. With the exception of JM46 and JM47, whose concentrations ranged from 0.25 to 8 $\mu\text{g/ml}$, all CORMs were tested with concentrations going from 2 to 32 $\mu\text{g/ml}$. 46

Individual columns in each graph represent the period of incubation: 24, 48 and 72 hours.
Cell viability was determined relatively to untreated cells.

List of Tables

Table 1.1 Properties and pharmacological action of the most relevant CORMs. Adapted from Motterlini <i>et al.</i> (2005) and Gullotta <i>et al.</i> (2012).	11
Table 2.1 List of equipment used throughout the present work, in alphabetical order.	17
Table 2.2 List of reagents used throughout the present work, in alphabetical order.	17
Table 2.3 List of CORMs, ligands and respective solvents used in this study.	18
Table 2.4 CORMs and ligands and concentrations tested in Gram-positive and Gram-negative bacteria.	20
Table 2.5 Minimum and maximum concentrations of each compound administered to LLC-PK1 cells in the MTT assay.	25
Table 3.1 List of CORMs organised by metal-centre in an alphabetical order.	27
Table 3.2 List of CORMs organised by respective ligands in alphabetical order.	28
Table 3.3 Minimum Inhibitory Concentrations of the 26 compounds under study, for <i>Staphylococcus aureus</i> and <i>Salmonella enterica</i> , expressed in µg/ml.	29
Table 3.4 Percentage of survival of <i>E. coli</i> , <i>S. aureus</i> and <i>S. enterica</i> upon treatment with JM46, JM20, JM47, JM20R, clotrimazole and CORM-3 for 2 and 4 hours.	33
Table 3.5 Percentage of survival of <i>E. coli</i> , <i>S. enterica</i> and <i>S. aureus</i> upon administration of the indicated CORMs and ligands.	36
Table 3.6 Carbonmonoxy-myoglobin (Mb-CO) formed, throughout time of incubation of Mb with the complexes JM46, JM20, JM47 and JM20R, expressed in µM.	41
Table 3.7 Half maximum inhibitory concentration of the compounds against LLC-PK1, after incubation for 24, 48 and 72 hours, expressed in µg/ml.	47
Table 4.1 Concentrations of CORMs that kill <i>E. coli</i> and <i>S. aureus</i> under aerobic conditions, from Nobre <i>et al.</i> (2007) ⁴⁶ .	49
Table S1 Percentage of survival of <i>Escherichia coli</i> over the course of 24 hours of incubation with 35 µM of JM46, JM20, JM47, JM20R, clotrimazole and 1 % of DMSO.	65
Table S2 Percentage of survival of <i>Salmonella enterica</i> over the course of 24 hours of incubation with 35 µM of JM46, JM20, JM47, JM20R, clotrimazole and 1 % of DMSO.	65
Table S3 Percentage of survival of <i>Staphylococcus aureus</i> over the course of 24 hours of incubation with 10 µM of JM46, JM20, JM47, JM20R, clotrimazole and 1 % of DMSO.	65

List of Abbreviations

A	Akt	Protein kinase B
B	Bcl-2	B- cell lymphoma 2 protein
	BVR	Biliverdin reductase
	BODIPY	Boron dipyrromethene difluoride
C	CDC	Centre for Disease Control and Prevention
	cGMP	Cyclic guanosine monophosphate
	CO	Carbon monoxide
	COP-1	Carbon Monoxide Probe 1
	CORM	Carbon Monoxide Releasing Molecule
D	DMSO	Dimethyl sulfoxide
	DMEM	Dulbecco's modified Eagle's medium
E	eNOS	Endothelial nitric oxide synthase
	ET-CORM	Enzyme Triggered – Carbon monoxide releasing molecule
	FBS	Foetal bovine serum
G	GI	Gastrointestinal
H	HAIs	Hospital acquired infections
	HO	Haem oxygenase
	HepG2	Human hepatocyte carcinoma cell line
I	IL-1β	Interleukin 1 β
	IC₅₀	Half maximum inhibitory concentration
L	LA	Luria Agar
	LB	Luria Broth
	LLC-PK1	Porcine kidney epithelial cell line
	LPS	Lipopolysaccharides
M	MAPK	Mitogen-activated protein kinase
	MHB	Muller Hinton Broth
	MIC	Minimum Inhibitory Concentration
	MRSA	Methicillin-resistant <i>Staphylococcus aureus</i>
	Mb-CO	Carbonmonoxy-myoglobin
	MTT	Thiazolyl Blue Tetrazolium Bromide
N	NALP3	NACHT, LRR and PYD domains-containing protein 3
	NARSA	Network on Antimicrobial Resistance in <i>S. aureus</i>
P	PAMP	Pathogen Associated Molecular Pattern
	PABA	Para-amino benzoic acid
	Pen-Strep	Penicillin-streptomycin

	PBS	Phosphate-buffered saline
R	ROS	Reactive Oxygen Species
	RAW	Murine macrophage cell line
S	sGC	Soluble Guanylyl Cyclase
	SLAM	Signalling Lymphocytic Activation Molecule
T	TLR4	Toll-like receptor 4
	TNF-α	Tumour Necrosis Factor α
	TSA	Tryptic Soy Agar
	TSB	Tryptic Soy Broth
U	UPEC	Uropathogenic isolates of <i>E. coli</i>
V	VISA	Vancomycin Intermediate-resistant <i>Staphylococcus aureus</i>
	VRSA	Vancomycin-Resistant <i>Staphylococcus aureus</i>
W	WHO	World Health Organization

1 Introduction

1.1 Carbon Monoxide

Carbon monoxide (CO) is a colourless, odourless and tasteless diatomic molecule, gaseous at room temperature, that shows hormesis, and which is of interest from a pharmacological point of view¹. The general population is exposed to CO on a daily basis since it is a product of the incomplete combustion of fuels that contain carbon, such as gasoline, natural gas, coal and wood. The majority of CO related accidents occur in households during the cold season. When inhaled at low concentrations or for a short period of time, CO can be asymptomatic. However, the severity of the symptoms depends on the dose and time frame of the exposure. A person may experience symptoms that vary from visual disturbance, seizures, coma, and ultimately, it can lead to death (Figure 1.1)².

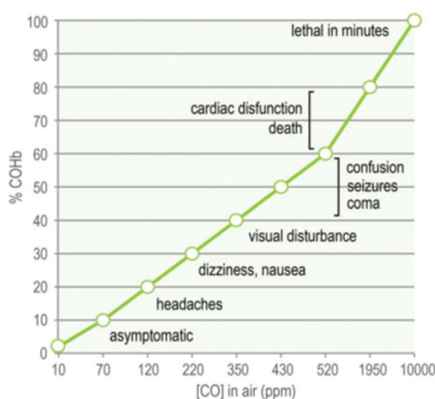


Figure 1.1 Carbon monoxide poisoning symptoms, in function of the concentration in the inhaled air. Reprinted from Romão *et al.* (2012)³

Carbon monoxide is produced endogenously by mammals, through the degradation of haem catalysed by haem oxygenase (HO). In humans there are three isoforms of this enzyme: HO-1, which is inducible by oxidative stress and haem release; HO-2, that is constitutively produced; and HO-3, that is a poor haem oxygenase most likely being a gene regulator of proteins like HO-1⁴⁻⁵. HO decomposes haem to biliverdin IXa, free iron and CO. Biliverdin is converted to bilirubin and the free iron is scavenged by ferritin (Figure 1.2). Some of the final products of HO catalysis were shown to be antioxidants, which supports the proposal that HO is essential to protect human cells from oxidative stress. In agreement, the promoter of HO-1 is activated in the presence of oxidative stimuli, like UV-radiation or haem⁶.

Under physiological conditions, CO occupies about 1 % of haemoglobin's binding sites, thus spreading throughout the mammalian circulatory system. When CO is present in the circulatory system at concentrations lower than 1 %, haemoglobin is mainly bound to oxygen. Therefore, the gas exchange in the lungs results in CO exhalation and consequent detoxification of

the CO produced endogenously⁷. However, an environmental increase in CO leads to an augment of its concentration in the blood stream. Consequentially the oxygen tension in the blood stream drops since there is a decrease in the amount of oxygen in the circulatory system. In this situation, the haemoglobin binds to CO. Therefore, the dissociation of CO from haemoglobin becomes more difficult which impairs CO detoxification with concomitant hypoxia. This poisoning effect is aggravated in tissues due to the higher affinity of myoglobin to CO than haemoglobin⁸.

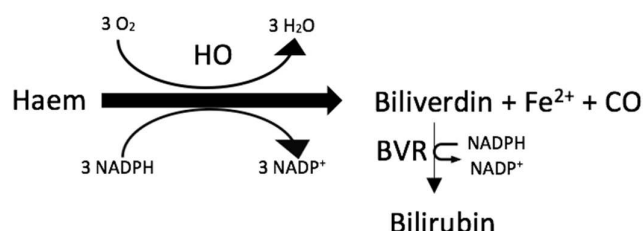


Figure 1.2 Catalytic mechanism of haem oxygenase. Haem is degraded by haem oxygenase (HO), originating biliverdin, free iron (Fe^{2+}) and carbon monoxide (CO). Biliverdin is then converted to bilirubin by biliverdin reductase (BVR).

In 1991, carbon monoxide was first described as an important messenger of the human body. Its ability to bind ferrous centres allows this molecule to activate the soluble guanylyl cyclase enzyme, sGC, which in turn produces cyclic guanosine monophosphate, cGMP. The production of cGMP has various effects in the human body, including cGMP-dependent protein kinase activation, smooth muscle relaxation and low platelet aggregation⁹⁻¹⁰. It was demonstrated that CO has a strong effect on the development of the neural network by augmenting the number of sodium channels¹¹. Other ionic channels, like calcium channels, seem also to be affected by CO¹². Furthermore, it has been shown that cells overexpressing HO-1 appear to be less likely to enter apoptosis when under stress. Additionally, it was demonstrated that CO is able to activate p38 mitogen-activated protein kinase, MAPK, on neighbouring cells, inhibiting apoptosis^{6,13}.

Carbon monoxide has been used in packaging of meats to improve its visual appearance, since the gas binds to myoglobin making the meat more red. It has been noticed that in this type of packaging, fewer pathogens were found when compared with other packaging systems, demonstrating the bactericidal effect of CO¹⁴. In the human body, CO is important to fight infections because it augments the immune response (Figure 1.3). By binding to the inner membrane respiratory complexes in bacteria, CO inhibits respiration. It has also been proposed that CO is able to induce adenosine triphosphate, ATP, production. ATP acts as a pathogen associated molecular pattern, PAMP, by activating P2X₇, a pattern recognition receptor, resulting in NALP3 inflammasome activation and IL-1 β secretion, leading to an increase of the immune response¹⁵.

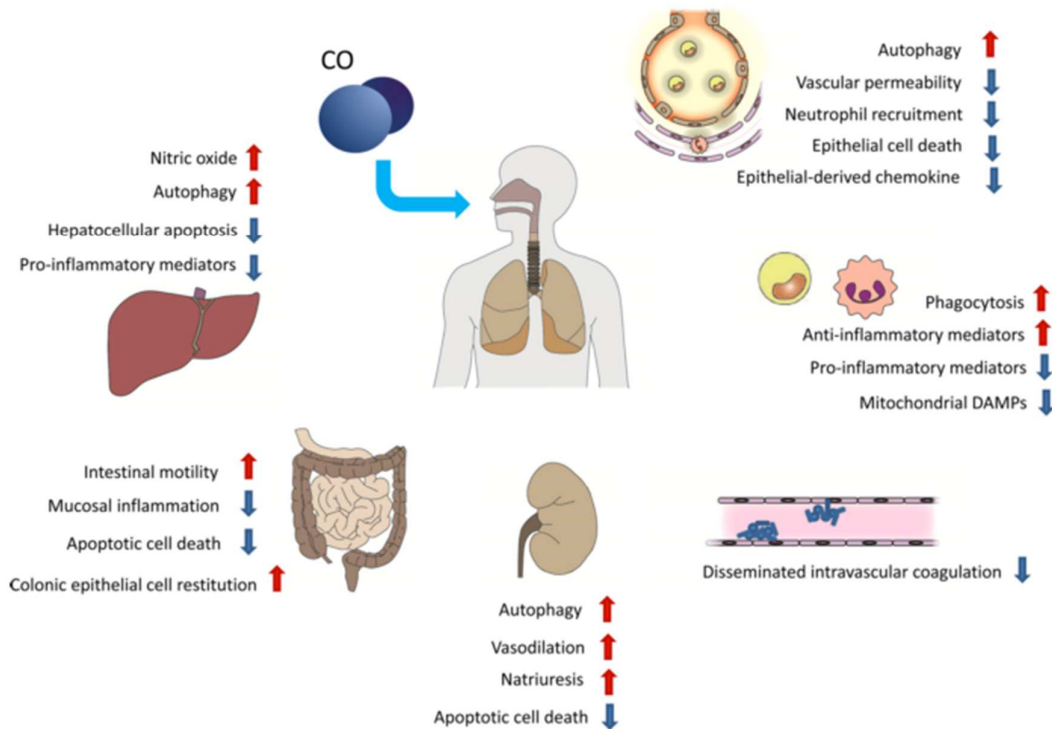


Figure 1.3 Schematic representation of the effects of CO on different areas of the organism. Reprinted from Nakahira *et al.* (2015)¹⁹

1.2 Carbon monoxide therapies

Several studies using animal models have demonstrated the benefits of a slight increase of the CO concentration in the inhaled air. Fujita *et al.* revealed that after ischemic stress, CO gas administration could prevent death of mice deficient in HO-1. Furthermore, in non-HO-1 deficient mice, the decrease of lethality observed upon CO supplementation by inhalation indicates that the amount of CO produced endogenously is insufficient to confer protection. Additionally, it was reported that CO potentiates fibrinolysis, which is related to ischemia recovery¹⁶.

Nakao *et al.* demonstrated that when CO gas is administered to rats after intestine grafts, it protects from ischemia through sGC activation. Moreover, when a sGC inhibitor was used, the beneficial effects of CO were no longer visible. Furthermore, it was observed the decrease of the pro-apoptotic factors, increase in anti-apoptotic like Bcl-2, and the activation of p38MAPK pathway, which altogether resulted in the decline of the inflammatory process¹⁷.

In 2004, rats were treated with CO gas in sub-lethal doses (250, 500 and 1000 ppm) for 24 hours before cardiac ischemia-reperfusion surgery. A reduced number of macrophages and

monocytes were found to migrate to the affected areas, together with a decrease of expression of the tumour necrosis factor alpha, TNF- α , which is involved in inflammation processes. The rats that had been pre-treated with 1000 ppm of CO presented a lower ratio of infarct areas to risk areas than the untreated rats and those that were exposed to 250 and 500 ppm. CO successfully improved rats' conditions, via p38MAPK and Akt-eNOS pathways, by the production of cGMP and nitric oxide (NO). Nevertheless, it is possible that these results are due to tissue hypoxia and its consequent effects¹⁸.

More recently, it has been proposed that CO may constitute a good treatment for sepsis, a systemic infection and inflammation¹⁹. CO up-regulates the signalling lymphocytic activation molecule, SLAM receptor, which is involved in the activation of hematopoietic cells that promote phagocytosis of Gram-negative bacteria and seems to be dependent on the presence of Beclin-1, a protein involved in autophagy (Figure 1.3)^{20,21}.

1.3 Bacteria

1.3.1 *Escherichia coli*



Figure 1.4 Scanning electron microscope photography of *Escherichia coli*. Reprinted from scharfphotography.com²².

First described as *Bacterium coli commune* by Theodor Escherich in 1885, *Escherichia coli* is a Gram-negative rod-shaped bacterium that is present in the gastrointestinal tract of humans and several animals²³. It was one of the first organisms to have its genome sequenced, and it is commonly used as a model organism, especially the K12 MG1655 strain²⁴. In fact, this bacterium is of great importance for humans as it has been shown that, under anaerobic conditions, *E. coli* is responsible for the production of menaquinones in the intestine. Menaquinones are the source of

vitamin K, which is essential for the clotting cascade. Therefore, people with high intake of antibiotics per year, present an impairment of the microflora and are prone to clotting problems²⁵.

Escherichia coli is an important pathogen with several strains responsible for infectious diseases. Furthermore, it is a good model organism of Gram-negative bacteria.

Pathogenic *E. coli* strains are accountable for diseases such as diarrhoea, meningitis, urinary infections and genital infections²⁶. *E. coli* strains may also cause bloodstream infections, are the leading cause of community and hospital-acquired urinary tract infections and are often associated with contaminated food²⁷. It is the main Gram-negative acquired pathogen in hospitals and communities, being very predominant in Europe. Southern Europe has the highest prevalence of resistant *E. coli* strains, maybe due to the lack of preventive measures and higher antibiotic prescription frequency²⁶. Usually, commensal bacteria do not cause intestinal infections. However, when these bacteria are displaced from their location, for example through a urinary catheter, and encounter a new location, an infection is established. Gastrointestinal infections are due to enteropathogenic *E. coli*. In rare occasions, a commensal bacterium turns pathogenic, so most infections are from externally acquired *E. coli* pathogenic strains²⁸. Some strains of *Escherichia coli* are not treatable by several antibiotics such as penicillins, quinolones, aminoglycosides, and may transfer plasmids containing resistance genes to other bacteria.

1.3.2 *Salmonella enterica*

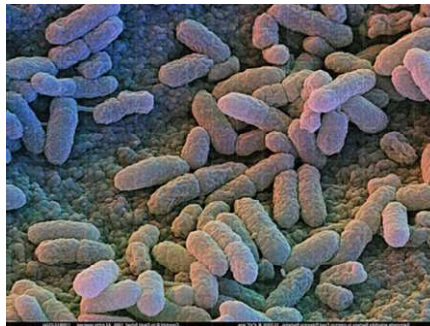


Figure 1.5 Scanning electron microscope photography of *Salmonella enterica*. Reprinted from scharfphotography.com²².

Salmonella is a Gram-negative rod-shaped bacterium, facultative anaerobe that ferments lactose and produces hydrogen sulphite. These bacteria can be transmitted through faecal matter and contaminated foods and vegetables, as its primary habitat is the intestinal tract of humans and farm animals. *Salmonella* can also be found in static waters as it forms biofilms and lays at the water surface. The most common food vehicles include raw eggs and chicken, therefore the

importance of well-cooked poultry food products. The danger in *Salmonella* is its ability to colonise easily a variety of hosts, facilitating infection from contact with pets or livestock^{29,30}.

There are two main species in the *Salmonella* genus: *Salmonella enterica* and *Salmonella bongori*. *S. enterica* can even be subdivided into six sub-species: *enterica*, *salamae*, *arizonae*, *diarizonae*, *houtenae*, and *indica*. *Salmonella* Typhi, a serovar of *S. enterica*, is one of the most harmful species. It can cause septicaemia and typhoid fever, which are very severe diseases that cause thousands of deaths in Asia every year. Other serotypes of *S. enterica* like Typhimurium, Enteritidis, Newport and Heidelberg are usually originated from food, and responsible for several hospitalisations and deaths per year²⁹. This pathogen causes Salmonellosis after colonising the intestinal epithelium and has been used as a biological weapon in several occasions. The symptoms may occur after 8 hours of ingestion and include headaches, vomit, chills, diarrhoea, and fever that may last several days³¹.

1.3.3 *Staphylococcus aureus*

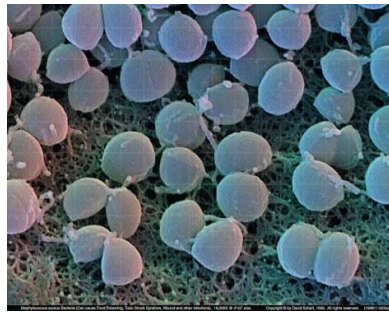


Figure 1.6 Scanning electron microscope photography of *Staphylococcus aureus*. Reprinted from scharfphotography.com²².

Staphylococcus aureus is a Gram-positive bacterium that colonises the human skin and nose²⁷. It is the most virulent staphylococci, being responsible for several serious infections. This bacterium is present in skin, oropharynx, gastrointestinal and urogenital tracts, and in immunocompromised hosts may originate infections that range from mild to life-threatening. It grows under aerobic and micro-aerobic conditions, with an optimum growth temperature of 37 °C, and forms round, raised yellow-golden colonies when grown in solid media. *S. aureus* virulence factors include toxins and enzymes that allow its invasion and spread into the host. Some of the *S. aureus* toxins are: α -toxin, β -toxin, γ -toxin, δ -toxin, leucocidin, exfoliative toxins A and B, toxic shock syndrome toxin-1 and enterotoxins. *Staphylococci* enzymes include coagulase, catalase, hyaluronidase, fibrinolysin, lipase, nuclease and penicillinase. Some *S. aureus* have capsules, that allows the pathogen to evade the immune system, and the majority of the strains express protein A that inhibits antibody-mediated immune response by binding to immunoglobulins³².

Over the years, *S. aureus* strains with resistance for several antibiotics have been emerging, including to β -lactams, generating a major health problem as these strains cause thousands of infections worldwide³³. The first methicillin-resistant *Staphylococcus aureus* (MRSA) appeared in 1962, just two years after the introduction of methicillin into the market. It is considered a serious threat by the Centre for Disease Control and Prevention (CDC) of the United States of America and the World Health Organization (WHO)^{27,34}. These strains are usually treated with vancomycin; however, in 1997 a MRSA tested for vancomycin presented a minimum inhibitory concentration (MIC) of 3-8 $\mu\text{g/ml}$ *i.e.*, it was no longer susceptible and constituted the first vancomycin intermediate-resistant *Staphylococcus aureus* (VISA)³⁵. This vancomycin-resistant *Staphylococcus aureus* (VRSA) was firstly reported approximately thirty years after the use of the drug. VRSA strains are also resistant to other antibiotics like methicillin; however, since so far few VRSA strains have been detected, it is not yet a serious threat³⁴.

1.4 Antibiotic Resistance

An antibiotic is a drug that is usually originated from a bacteria or fungi and that inhibits the growth of other bacteria. It can be synthetically altered and is less-toxic to humans and animals than to bacteria. It differs from an antiseptic (topical use) and disinfectant (surface use) since it can be ingested. The first antibiotics appeared in the 1930's and were sulphonamides. These compounds inhibit the production of folic acid by the bacteria, causing their death. Bacteria produce their own folic acid, whereas humans obtain it from the diet. By inhibiting the production of folic acid, bacteria are unable to produce DNA and RNA, which causes their death³¹. Even though Fleming discovered penicillin in the summer of 1928, only in 1938 a group of English scientists would develop a protocol to produce large amounts of the antibiotic, saving hundreds of injured soldiers of the Second World War. Not long after, in 1946, the first penicillin resistant bacterium was found³⁶. Moreover, in the recent years, the rate of resistant bacteria has been increasing due to the large amount of antibiotics used worldwide not only in humans but also in cattle and for agriculture purposes²⁶.

There are 5 major families of antibiotics: β -lactams, tetracyclines, aminoglycosides, macrolides and quinolones. Beta-lactams, like penicillins and cephalosporins, inactivate some of the enzymes responsible for the cell-wall formation. Tetracyclines block bacterial protein production impairing cell growth and division. Aminoglycosides, like streptomycin and kanamycin, prevent protein synthesis originating deficient proteins. Macrolides, like erythromycin and azithromycin also inhibit protein synthesis. Finally, quinolones target bacterial DNA. Some other currently available antibiotics are not included in any family, such as rifampicin that prevents transcription³⁶.

Antibiotic-resistant bacteria are usually due to mutations that confer bacteria the ability to overcome the toxic effect of the antibiotic. A mutation can occur in 1 bacterium in a pool of 10 million; as during a bacterial infection billions of pathogenic cells invade the host the occurrence of antibiotic-resistance mutations is very high. Furthermore, the repeatedly use of antibiotics worldwide allow the spread of these mutations due to a Darwinistic effect²⁶.

Some of the mechanisms that sustain bacterial resistance are the production of new or altered enzymes that can obstruct the antibiotic or the antibiotic target. A well-known example is β -lactamase, a bacterial enzyme that degrades β -lactamic acid. However, in order to overcome this resistance new drugs were designed containing a mixture of β -lactams and clavulanic acid, an inhibitor of β -lactamase³⁶.

Another strategy used by bacteria is the deactivation of the antibiotic. For example, some bacteria promote addition of a chemical group to streptomycin, which impairs its binding to the ribosome. Some other bacteria do the opposite, as they alter the ribosome by binding a methyl group which ceases to be targeted by the antibiotic³⁶.

Other antibiotic resistance mechanisms are: i) pumps that constantly expel antibiotics out of the cell-wall, for example in *Pseudomonas aeruginosa* (*P. aeruginosa*) that pump tetracyclines and other antibiotics; ii) production of an excess substrate or target of the antibiotic. An example is overproduction of para-amino benzoic acid (PABA), the substrate of the enzyme that is targeted by sulphonamides, which when in excess in the cytoplasm, it is more likely that the enzyme will bind to PABA than to the sulphonamide. Furthermore, several Gram-negative bacteria, such as *P. aeruginosa* and *E. coli* are known to be able to reduce their membrane permeability, which makes them resistant to several types of antibiotics³⁶.

Another type of antimicrobials are imidazoles, such as clotrimazole and miconazole that are antifungals. Interestingly, these compounds are also effective against Gram-positive bacteria including staphylococci³⁷. In *S. aureus*, binding of imidazoles to flavohaemoglobins produces reactive oxygen species (ROS) that originate oxidative stress. In agreement with these results, another study showed that flavohaemoglobin deficient mutants of *Staphylococcus aureus* were less susceptible to imidazoles³⁸.

The misuse of antibiotics, including as a prevention method, and the presence of antibiotics in animal food, and for cattle growth are factors that contributed to a situation where it is not easy to predict the consequences of the current spreading of resistant bacteria. This behaviour contributes to the appearance of more lethal bacterial strains. It becomes urgent to search for different and more efficient antibiotics to overcome the multifactorial bacterial defence mechanisms³⁶.

1.5 Carbon Monoxide Releasing Molecules (CORMs)

Carbon monoxide releasing molecules (CORMs) are, in general, metal carbonyl complexes with a central transition metal like ruthenium or manganese and, at least, one CO group as coordinated ligand. These compounds are able to deliver CO in a controlled and targeted way to cells and tissues. This study will focus on metal carbonyl-based CORMs that are the best studied ones and have been demonstrated to be the most suitable molecules to fulfil therapeutic purposes. Additionally, the presence of other ligands may intensify the CORMs action.

Although the administration of CO can be done in the form of gas or by a transporter molecule (Figure 1.7), the amount of CO required to achieve beneficial concentrations in the tissues would reach lethal doses. Moreover, CO is not site specific, resulting in concentrations lower than the ones required in the target areas, and very high concentrations of CO in unwanted regions of the organism.

CORMs have revolutionised the CO therapy as these molecules can be built with tissue specificity as well as biological action (Figure 1.8). Importantly, CORMs are predicted to transport CO throughout the body without interference of haemoglobin, the oxygen transport and delivery system of mammals. Once reaching the target, the CO group may be liberated from the molecule spontaneously or by specific conditions^{39,40}.

Some CORMs only release CO under specific conditions, which may be helpful when constructing an organ specific molecule.

In particular, photo-CORMs are radiation-dependent, meaning that they liberate CO when irradiated by specific wavelength radiation. These CORMs can be used for topical application, upon activation by sunlight or another light source.

ET-CORMs are enzyme-dependent and only liberate CO after cleavage by a specific enzyme. These CORMs can be used to target organs that contain a particular enzyme.

Lastly, pH-dependent CORMs that liberate CO at a specific pH, can be used in organs such as the stomach or the bladder that have pH very distant from the blood.

Motterlini and his team developed the first CORM in 2001, namely $[\text{Mn}_2(\text{CO})_{10}]$ designated as CORM-1, a CORM that is photo-activated and aimed to treat several physiological alterations (Table 1.1). Later, the group developed CORM-2 that is soluble in dimethyl sulfoxide (DMSO), and CORM-3 that is soluble in water and, consequentially, more suitable to pharmacological use. More recently, Nobre *et al.* reported that even at high concentrations CORM-2 and CORM-3 are not toxic to murine macrophages RAW 264.7, porcine kidney LLC-PK1 and human liver HepG2⁴¹. Motterlini *et al.* showed that CORM-1 to 3 liberate CO by measuring the concentration of CO bound to

myoglobin spectrophotometrically (the so-called myoglobin assays), with CORM-3 being one of the fastest CO releasers⁴⁰. Nobre *et al.* have also demonstrated, using a specific carbon monoxide probe-1 (COP-1) that CORM-2 releases CO to the intracellular space of bacterial and eukaryotic cells⁴¹. Furthermore, Davidge *et al.* demonstrated that CO liberated from CORM-3 is incorporated by bacterial cells since when in the presence of *E. coli* the percentage of CO attached to myoglobin is much lower⁴².

Not long ago, CORM-2 was considered a possible treatment for acute pancreatitis. In a study using human and mice monocytes and macrophages, where the compound was able to ameliorate the inflammatory cascade, CORM-2 was shown to induce anti-inflammatory cytokines and inhibited the TLR4 receptor⁴³.

CORM-3 administration to rats led to the *in vivo* release of CO that activates sGC, potentiating vasodilatation, and such effect is impaired by addition of myoglobin or a guanylyl cyclase inhibitor. It was also observed that the effects of CORM are long-lasting and for some concentrations can overcome the guanylyl cyclase inhibitor, most probably due to CO competition to the inhibitor⁴⁴.

Nowadays CORM-2 and CORM-3 remain the best studied and more used CORMs in research.

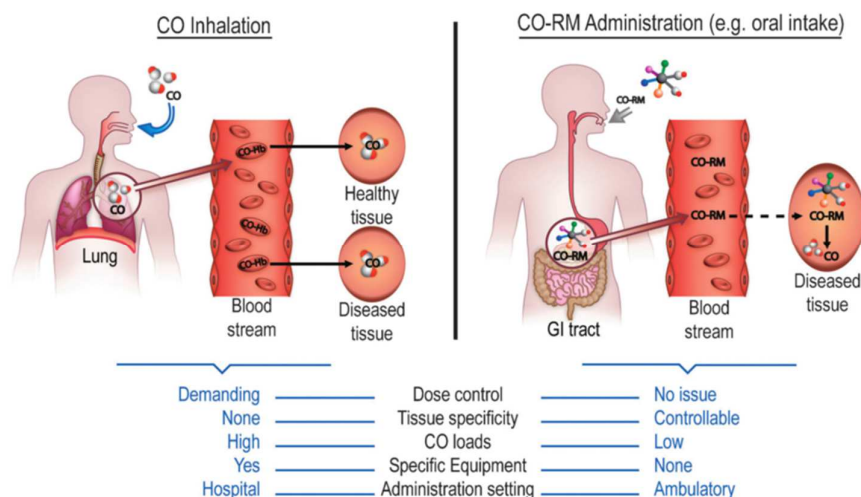


Figure 1.7 Carbon monoxide administration methods and their advantages. Reprinted from Romão *et al.* (2012)³.

More recently, Romanski *et al.* have synthesised acyloxybutadiene–iron tricarbonyl complexes, which are designated as ET-CORMs. These complexes are relatively stable, and only release their three CO molecules after entering cells due to cleavage of the compound by

esterases and degradation by oxidative decomposition. In lipopolysaccharide (LPS) stimulated murine macrophages, one of the compounds designated as rac-13, was shown to impair NO production by 68 % at concentrations of 15 μM . Even though the compound presented some cytotoxicity towards animal cells, the concentration needed for 30 % inhibition of NO production was very low, and this CORM showed no associated cytotoxicity. ET-CORMs opened the possibility to construct a molecule that is cleaved by specific enzymes, with putative function for targeting specific organs and possibly that even if it is homogeneously distributed throughout the body, the CORM will only act upon the desired location⁴⁰.

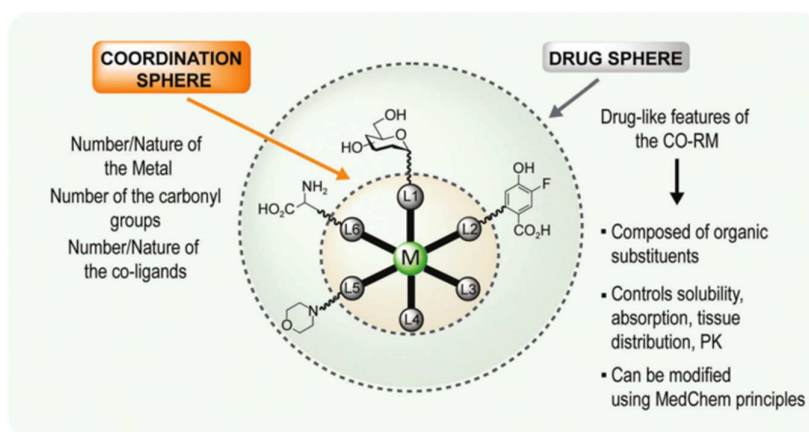
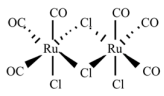
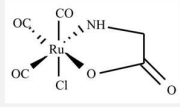


Figure 1.8 Schematic representation of the construction of CORMs for pharmacological purposes. M represents the metal centre and L1-L6 can be substituted by functional ligands or CO groups. Reprinted from Romão *et al.* (2012)³.

Table 1.1 Properties and pharmacological action of the most relevant CORMs. Adapted from Motterlini *et al.* (2005) and Gullotta *et al.* (2012)^{39,45}.

Compound	Chemical Structure	Solubility	CO release (in PBS, pH= 7.4, 37 °C)	Pharmacological action	Year of identification
CORM-1		DMSO Ethanol	Light dependent Fast ($t_{1/2} < 1$ min) 1 M CO/mole CO-RM	Vasodilator Reno-protective	2001

CORM-2		DMSO Ethanol	Induced by ligand substitution Fast ($t_{1/2} \approx 1$ min) 0.75 M CO/mole CO-RM	Vasodilator Reno-protective Anti-inflammatory Anticarcinogenic Proangiogenic Antiapoptotic Antiproliferative Bactericidal	2002
CORM-3		H ₂ O (stable at acidic pH)	Induced by ligand substitution/water-gas shift reaction Fast ($t_{1/2} \approx 1$ min) ≈ 1 M CO/mole CO-RM	Vasodilator Reno-protective Cardio-protective Anti-inflammatory Anti-ischemic Antiplatelet aggregation Bactericidal	2003

1.5.1 Carbon monoxide releasing molecules as bactericides

In 2007, Nobre *et al.* showed that CORMs are also antimicrobial agents. It was demonstrated that CO gas, CORM-2 and CORM-3 impair the growth of *E. coli* and *S. aureus*. The water-soluble CORM-3 was shown to be more toxic to *E. coli* than to *S. aureus*, namely under aerobic conditions, and less active than CORM-2. In fact, the MIC of CORM-3 is 400 μ M for *E. coli* and 500 μ M for *S. aureus*, whereas for CORM-2 the MICs are 350 μ M and 250 μ M, respectively^{41,46}. These results were proven to be dependent on the presence of the CO molecule in the CORM structure, since when a CO scavenger such as haemoglobin was added, the growth was restored⁴⁶.

Another CORM tested by Nobre *et al.* was ALF062, a molybdenum-based CORM, which strongly affected the growth of *E. coli* and *S. aureus*. Even though ALF062 liberates some CO to the culture medium, contrarily to CORM-2 and CORM-3, the authors proposed that a significant number of molecules penetrate the cell wall and liberate the CO to the cytosol, and that in the presence of haemoglobin the growth impairment was cancelled. In fact, exposure to ALF062 resulted in accumulation of molybdenum inside *E. coli* cells that was not detected in the control cells. Furthermore, the decomposition products of ALF062 did not impair bacterial growth confirming that the presence of the CO chemical entity was required for the bactericidal action. In

general, these results showed that CORMs are more effective under low oxygen concentrations, which also means that the growth inhibition is not only due to the impairment of the respiratory chain by the binding of CO to the oxygen reductases⁴⁶.

Davidge *et al.* later reported that CORM-3 impairs *E. coli* growth at concentrations of 30 μM , under aerobic conditions, and at 200 μM , under anaerobiosis. Interestingly, when a similar experiment was conducted with a CO saturated solution instead of CORM-3, with similar final CO concentrations, no impairment was observed. This indicates that, for the same concentration of CO, the gas itself is insufficient for bactericidal activity. When using a CORM-3 molecule with coordinated DMSO instead of CO groups, no bactericidal activity was also observed. When the authors performed a staining assay that permitted to distinguish between live and dead cells (LIVE/DEAD™ staining assay) they observed that under aerobic conditions the reduction of live/healthy cells was of 48 %, while under anaerobic conditions CORM-3 did not reduce the percentage of live cells⁴².

Bang *et al.* reported that bacteria exposed to CORM-2 at the stationary phase were less inhibited than those exposed at the exponential phase, indicating that cells with higher metabolic activity are more susceptible to CORM-2. The authors also proposed that while at stationary phase bacteria may represent dormant persisters, with a temporarily resistance to CORM-2⁴⁷.

The transcriptomic analysis of the effect of CORM-2 on *E. coli* revealed the CORMs' targets. *E. coli* grown aerobically and exposed to CORM-2 caused the repression of genes involved in coenzyme catabolic processes, tricarboxylic acid cycle and aerobic respiration classes which indicates an inhibition of aerobic respiratory processes⁴⁸. Additionally, CORM-2 induces the expression of the gene *recA* and causes damage of bacterial DNA⁴⁹.

E. coli cells treated with CORM-2 and grown anaerobically had the transcription of 228 genes repressed, the majority of these genes being involved in amino acid transport and metabolism⁴⁸. In particular, CORM-2 enhanced the transcription of *ftnB*, a gene encoding ferritin-like protein, and the expression of genes involved in sulphur and methionine metabolism⁴⁸. Additionally, it is known that methionine deficient bacteria have an increased oxidative stress, which also occurs after the exposure of bacteria to CORMs^{41,50}. Moreover, CO can displace histidine, cysteine and tyrosine residues from metal centres in molecules, which can alter the protein⁵⁰.

Nobre *et al.* reported that under aerobic conditions *E. coli* cells treated with CORM-2, CORM-3 and ALF062 had increased intracellular ROS content, particularly, when exposed to CORM-2⁴¹. In agreement, Tavares *et al.* reported that *E. coli* in the presence of CORM-2 or CORM-3, leads to the upregulation of several genes encoding proteins involved in defence mechanisms, oxidative stress and protein homeostasis. Moreover, addition of CORM-3 to *E. coli*

cause that the released CO bound to terminal oxidases with consequent impairment of the respiratory chain reaction, which also contributes to increase the formation of intracellular ROS⁵⁰. Furthermore, studies revealed that susceptibility of *E. coli* to CORMs increases when genes encoding systems of ROS detoxification are mutated, and that addition of antioxidants impairs bacterial death⁴⁹.

In contrast with these results, *P. aeruginosa* didn't show any alterations after CORM-3 treatment, particularly H₂O₂ production, indicating that there is no ROS formation. Furthermore, *P. aeruginosa* grown in the presence of both CORM-3 and several antioxidants did not reverse the toxicity effect, therefore bactericidal effect against *P. aeruginosa* is most likely not related with oxidative stress⁵¹.

Increased biofilm production is a defence mechanism, associated with the virulence of the strains, since pathogenic strains augment the biofilm production, which is observed in the presence of several antimicrobial agents. Studies done with CORMs revealed that, when grown in Luria broth (LB) medium and in the presence of oxygen, *E. coli* cells produce about 2 times more biofilm⁴⁸. Bang *et al.* have demonstrated that CORM-2 also increases biofilm production in *E. coli* extended-spectrum β -lactamase producing isolate (ESBL) and in uropathogenic isolates of *E. coli* (UPEC). When a LIVE/DEAD™ staining assay was conducted for cells with a well-established biofilm, results have shown that CORM-2 effects are only visible after 24 hours of exposure. The authors also evaluated the bactericidal effect of CORM-2 in UPEC infected bladder epithelial cells, observing that CORM-2 significantly reduced bacterial counts after 4 hours of exposure, but not the CO-free analogue, suggesting that CO is contributing to the bactericidal activity⁴⁷.

Tavares *et al.* reported that CORM-2 accentuates the efficacy of the metronidazole antibiotic currently used to treat *Helicobacter pylori* (*H. pylori*) infections. In these experiments, six metronidazole resistant clinical strains of this pathogen were treated with CORM-2, metronidazole and both. Bacterial MIC of CORM-2 varied from 100 to 200 mg/L, whereas metronidazole MIC varied from 2 to 64 mg/L. When both CORM and antibiotic were given to the bacterial cultures the MIC values were significantly reduced, being the most evident the reduction of the metronidazole MIC for the clinical isolate 5611, that decreased from an initial MIC of 64 mg/L to 8 mg/L when administered together with 100 mg/L of CORM-2. Furthermore, the two antimicrobials were also tested in *H. pylori* infected macrophages. After combining 100 mg/L of CORM-2 with 1.5 mg/L of metronidazole, a reduction by about 98 % of the bacterial count was observed, which was significantly higher than the 30 % reduction observed when infected macrophages were treated with metronidazole alone⁵².

Recently, Simpson *et al.* developed a new type of CORM that combines a CORM and an antibiotic. Stable compounds in which Mn(CO)₃(N–N) moiety was coordinated to an azole, such as ketoconazole, miconazole and clotrimazole, were synthesised (their position is highlighted in yellow

in Figure 1.9)⁵³. These later antibiotics are antifungals, and clotrimazole in particular is a drug that inhibits the production of ergosterol and other sterols necessary for a proper formation of the extracellular membrane. When a cell membrane is compromised, there is an increased permeability to ions like H⁺ and K⁺, which can result in acidification of the cytosol and consequent activation of lytic enzymes⁵⁴.

The biological activity of the new CORMs was assessed in Gram-positive and Gram-negative bacteria, as well as in two parasites: *Leishmania major* and *Trypanosoma brucei*. The clotrimazole-CORM complex displayed the best activity against Gram-positive bacteria. The conjugation with the organometallic complex increased clotrimazole activity-fold 30 times⁵³.

Clotrimazole has also been coordinated to other metals like copper, cobalt, zinc and nickel, and tested in human carcinoma cells. The cytotoxicity of these complexes was higher than the clotrimazole alone, indicating that the coordination to the metal augmented the toxicity of the free ligand⁵⁵.

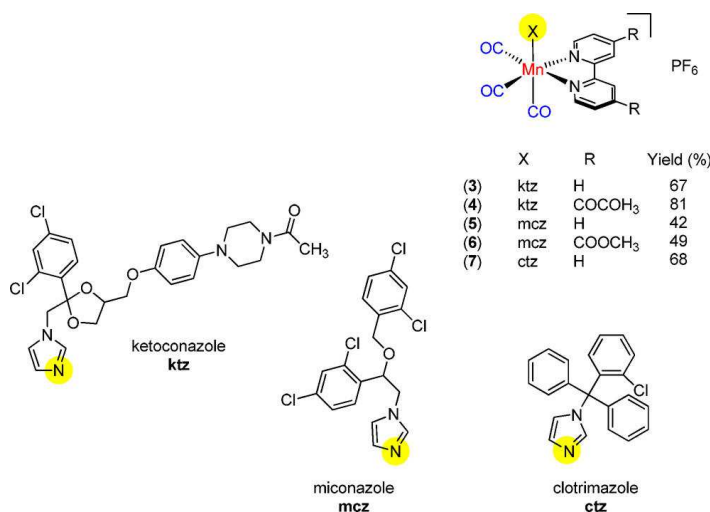


Figure 1.9 Organometallic molecule on the top right corner, and different coordination ligands at the bottom. The metal-coordinated atom is highlighted in yellow. Adapted from Simpson *et al.* (2015)⁵³

More recently, another photoCORM was described. Upon activation by UV light, the compound impairs bacterial growth and cell viability, to an extent greater than CO gas alone. Moreover, when compared with ruthenium-based CORMs, this manganese photoCORM has shown to be less toxic to animal cells⁵⁶.

1.6 Aim of this work

The general purpose of this work was to evaluate the bactericidal effect of novel CORMs (that have been produced in the laboratory of Professor Carlos Romão, ITQB-NOVA) and analyse their mechanism of action towards bacterial cells. These compounds are constituted by a metal centre coordinated by two or more CO molecules together with other ligands that help stabilise or improve their function. These CORMs can be organised in 3 families according to their metal centre. Some CORMs were combined with antifungals and their bactericidal activity was also tested.

Specifically, a total of 18 CORMs together with 8 organic ligands used for CORM-coordination and the respective solvents were evaluated. The following objectives of this work were successfully attained:

- i. Evaluate the bactericidal activity of CORMs in pathogenic strains;
- ii. Elucidate the mechanism of action of CORMs through different methodologies;
- iii. Evaluate the toxicity of CORMs to mammalian cells.

2 Materials and Methods

All the equipment and reagents used throughout the present work are described in tables 2.1 and 2.2, respectively.

Table 2.1 List of equipment used throughout the present work, in alphabetical order.

Equipment	Model	Manufacturer
Centrifuge	5810R	Eppendorf
Fluorescence Microscope	DM6000 B	Leica
Incubator	C 150	Binder
Inverted Microscope	Primo Vert	ZEISS
Microplate Spectrophotometer	Multiskan™ GO Microplate Spectrophotometer	Thermo Scientific™
Shaker	KS4000 ic control	IKA
UV-Vis spectrophotometer	UV-1603 spectrophotometer	Shimadzu

Table 2.2 List of reagents used throughout the present work, in alphabetical order.

Reagent	Manufacturer
2-Propanol	Honeywell
2,2'-Bipyridyl-4,4'-dicarboxylic acid	Sigma-Aldrich
Agar	Difco Laboratories (Becton, Dickinson and Company)
Clotrimazole	Sigma-Aldrich
CO gas	Linde
CO ₂ gas	Air Liquide
CORM-3	Sigma-Aldrich
Dulbecco's modified Eagle's medium	Gibco® by Life technologies™
DMSO	Carlo Erba Reagents
Fetal Bovine Serum	Gibco® by Life technologies™
LIVE/DEAD™ BacLight™ Bacterial Viability Kit	Invitrogen by Thermo Fisher Scientific
LLC-PK1 cell line	Sigma-Aldrich
Luria Broth	Carl Roth
Mueller-Hinton Broth	Sigma-Aldrich
Myoglobin from equine skeletal muscle	Sigma-Aldrich
Penicillin-Streptomycin	Gibco® by Life technologies™
Sodium Chloride	Fisher Scientific
Sodium hydrosulfite	Sigma-Aldrich

Thiazolyl Blue Tetrazolium Bromide	Sigma-Aldrich
Trypan Blue	Fluka
Trypsin	Corning™
Tryptic Soy Agar	Difco Laboratories (Becton, Dickinson and Company)
Tryptic Soy Broth	Difco Laboratories (Becton, Dickinson and Company)

2.1 CORMs, ligands and solvents

The CORMs, ligands and respective solvents used in this work are described in table 2.3. These 18 newly synthesised CORMs, when organised according to the metal centre represent 3 families of CORMs. Also, the 8 organic ligands used for CORM-coordination and the respective solvents were tested. With the exception of CORM-3, all the CORMs and the ligands marked with an asterisk in table 2.3 were synthesised by Joana Marques and kindly provided by Professor Carlos C. Romão, ITQB-NOVA.

Table 2.3 List of CORMs, ligands and respective solvents used in this study.

CORMs	Solvent
JM32, JM41, JM42	PBS
JM20	Methanol
CORM-3	H ₂ O
HL2, JM14, JM16, JM20R, JM46, JM47, JM60, JM62, JM69, JM80, JM94, JM97, JM106, JM107	DMSO
Ligand	Solvent
2,2'-Bipyridyl,	PBS
Tris(hydroxymethyl)phosphine	Methanol
1,10-Phenanthroline	H ₂ O
Pyridine-2-carboxaldehyde,	DMSO
Tetramethylethylenediamine	
Clotrimazole, JM108*, JM109*	

2.2 Bacterial strains and growth conditions

In the present work, three bacterial strains were tested namely two Gram-negative, *Escherichia coli* K12 MG1655 and *Salmonella enterica serovar* Typhimurium SL1344, and one Gram-positive, *Staphylococcus aureus* MRSA USA300 JE2.

The *E. coli* strain used was obtained from the host laboratory stock cultures. The *S. aureus* JE2, is a plasmid-cured strain derived from *S. aureus* USA300 LAC, a community-associated MRSA and was obtained from the Network on Antimicrobial Resistance in *S. aureus* (NARSA, Chantilly, VA, United States). The *S. enterica* bacterial strain was kindly provided by Professor Cecília Arraiano, ITQB-NOVA.

Stock cultures of bacterial strains were kept at -80 °C in Luria-Broth (LB) and Tryptic Soy Broth (TSB), for Gram-negative or Gram-positive respectively, with 25 % glycerol. When needed, stock cultures were plated onto petri dishes containing Luria Agar (LA) in the case of Gram-negative, or Tryptic Soy Agar (TSA) for Gram-positive bacteria, left at 37 °C overnight and the isolated colonies formed were stored at 4 °C, for a maximum of 3 weeks. For each growth assay, an isolated colony was inoculated into LB or TSB, for Gram-negative or Gram-positive respectively, and incubated overnight at 37 °C, 150 rpm.

The overnight grown cells were used to inoculate fresh media and cultured until reaching an OD_{600nm} of 0.1. Bacterial strains were treated with the compounds according to the conditions described in table 2.4. Untreated bacterial cultures and treated with 1 % (v/v) of the solvent used to dissolve the correspondent compound were also tested. Compounds were added when cells reached an OD_{600nm} of 0.3 and growth proceeded up to 24 hours and monitored as indicated in each case.

Table 2.4 CORMs and ligands and concentrations tested in Gram-positive and Gram-negative bacteria.

Compound	Gram-positive	Gram-negative
Clotrimazole		
JM20		
JM20R	10 μ M	35 μ M
JM46		
JM47		
CORM-3		
JM14		
JM16		
JM94		250 μ M
JM106		
1,10-phenanthroline		
2,2'-Bipyridyl		
DMSO		
Methanol		1 % (v/v)

2.3 Minimum Inhibitory Concentration assay

The minimum inhibitory concentration (MIC) is defined as the lower concentration at which a compound completely inhibits bacterial growth as to visual observation. It is usually done through a series of dilutions in a pre-defined scale, the two-fold dilutions being the most common (1, 2, 4, 8, ... 64, 128 μ g/mL)⁵⁷. For this experiment, Muller Hinton Broth (MHB) was used following the procedures recommended for the antibiotic susceptibilities studies by the Clinical and Laboratory Standards Institute, USA⁵⁸. This widely used media culture presents batch-to-batch reproducibility for several antibiotics, it is low on inhibitors and can be used with a wide range of pathogens⁵⁸.

Overnight grown bacterial cultures (37 $^{\circ}$ C, 150 rpm) were used to inoculate MHB to a final OD_{600nm} of 0.01. Aliquots of 200 μ l were then transferred to a 96 well-plate. Each compound was added to the cells and two-fold dilutions of the highest and lowest concentration (i.e. from 32 to 2 μ g/mL) were tested, with the exception of JM46 and JM47 which concentrations ranged from 0.25 to 8 μ g/mL. After 18 hours of incubation at 37 $^{\circ}$ C and 90 rpm, MICs were assessed by visual inspection of the wells' turbidity. Three independent biological samples were tested in triplicate (i.e. n=9).

2.4 Bacterial cell membrane permeability assay

The cell membrane permeability was assessed using the LIVE/DEAD® BacLight™ Bacterial Viability Kit, which is composed of two nucleic acid stains, SYTO™ 9 and propidium iodide. The green-fluorescent SYTO™ 9 dye is able to penetrate damaged and not damaged cell membranes, but the propidium iodide only crosses damaged membranes, promoting the displacement of SYTO™ 9 due to its higher affinity for nucleic acids, which causes a shifting of the cell staining from green to yellow-red colour. According to the manufacturer, a cell exhibiting a colour between light yellow and bright red, is considered dead or non-viable (Figure 2.1).

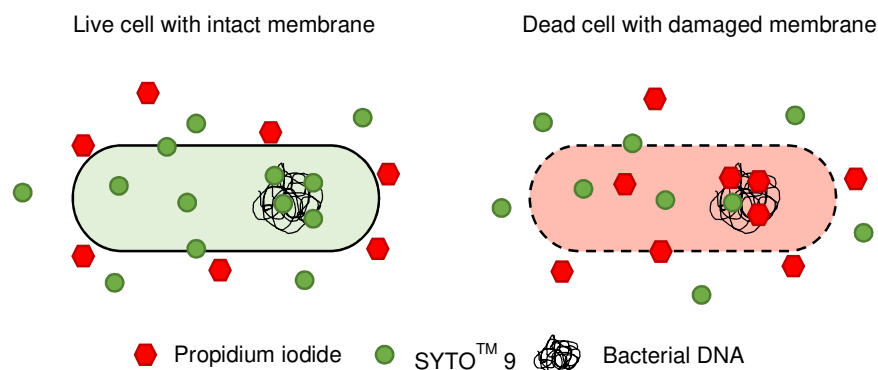


Figure 2.1 Cell membrane permeability assay. SYTO™9 (green circle) can enter all cells (live and dead) whereas propidium iodide (red hexagon) can only enter permeable cells (dead).

The experiments were conducted according to manufacturer instructions. For these assays, overnight grown cells were used to prepare bacterial suspensions in MHB with an OD_{600nm} of 0.1. Cells were then incubated until reaching an OD_{600nm} of 0.3, and at this stage JM46 and JM47 were added to a final concentration of 8 $\mu\text{g}/\text{mL}$ for Gram-positive bacteria and 32 $\mu\text{g}/\text{mL}$ for Gram-negative bacteria. After a 2 hours incubation at 37 °C, 150 rpm, the ODs were measured, and aliquots were collected in order to obtain cell suspensions of 333 μL , with an OD of 5, which were later loaded onto the microscopy slide (Equation 2.1).

Equation 2.1 . Volume of culture retrieved for the cell membrane permeability assay. The volume retrieved is represented by a v (μL) and the optical density of the culture at 600nm is represented by $OD_{culture}$.

$$v = \frac{5 * 333}{OD_{culture}}$$

The aliquots were centrifuged at 10000 $\times g$ for 10 minutes, and the supernatants were discarded. Samples were first washed with 1 mL of 0.85 % NaCl. The control sample for non-viable

cells staining was done by adding 1 ml of 70 % isopropanol to the first wash, instead of NaCl, in order to kill all bacterial cells. Samples were incubated again for 30 minutes at room temperature, and then washed with 0.85 % NaCl. According to the manufacturer's protocol, the dye mixture is added so that a final concentration of 0.3 % (v/v) is achieved. Therefore, for the addition of 1 μ L of a mixture of SYTOTM 9 and propidium iodide (1:1), the resulting pellets were resuspended in 333 μ L of NaCl and incubated at room temperature in the dark for 15 minutes.

Samples were loaded (3 μ l) onto slides previously prepared with 900 μ l of agarose 1.7 % (w/v). Samples were observed in a Leica DM6000B fluorescence microscope, with a phase contrast Uplan F1 100x objective and a CCD Ixon camera (Andor Technologies). All samples were excited at 488 nm with filter sets FITC and Texas RedTM, and the emission was collected by a META detector at 525 and 615 nm, for SYTOTM 9 and propidium iodide, respectively. For each experiment, 4 samples were observed in the microscope, namely a control of non-viable cells staining, untreated cells as control of live/healthy cells, and cells treated with JM46 and with JM47. Similar assays were done 24 hours after the addition of the compounds. The microscope images were analysed with the Metamorph software version 5.8 (Universal Imaging).

This experiment was performed three times on *E. coli*, *S. enterica* and *S. aureus*, and in each experiment each condition was tested in duplicate.

2.5 Detection of CO release from CORMs

2.5.1 Myoglobin assay

Oxidised myoglobin from equine skeletal muscle was first reduced by addition of sodium dithionite. Reduced myoglobin (Mb), exhibits a band at 555 nm in the Visible spectrum. Binding of CO released from CORMs to myoglobin results in the formation of carbonmonoxy-myoglobin (Mb-CO) whose spectrum displays two bands at 540 and 570 nm. By measuring the change in absorbance at 540 nm and using the Lambert-Beer Law ($\epsilon_{540} = 15.4 \text{ mmol/L}^{-1} \cdot \text{cm}^{-1}$), the amount of Mb-CO formed was determined⁴⁴.

Solutions of myoglobin and sodium dithionite were manipulated under anaerobic conditions; therefore, the chemicals were weighted in glass containers, encapsulated and air purged by means of an argon flux applied for 15 minutes. Previously deaerated PBS was added to the myoglobin using a purged syringe. The dissolved myoglobin (60 μ M) was immediately reduced by addition of the sodium dithionite. To prepare the control sample of Mb-CO, an aliquot of 1 mL of Mb, previously incubated for 15 minutes with sodium dithionite at room temperature, was placed under CO gas flux for 30 minutes. CORMs (60 μ M) were added to aliquots of 1 ml of reduced

myoglobin, transferred with a purged syringe to anaerobic quartz cuvettes and the spectrum immediately acquired. Spectrophotometric measurements were done at 37 °C every 30 minutes and over 2 hours. In total, 6 samples were measured spectrophotometrically, namely Mb, Mb-CO, and Mb in the presence of 60 μ M of JM20, JM20R, JM46 or JM47. This experiment was performed three times.

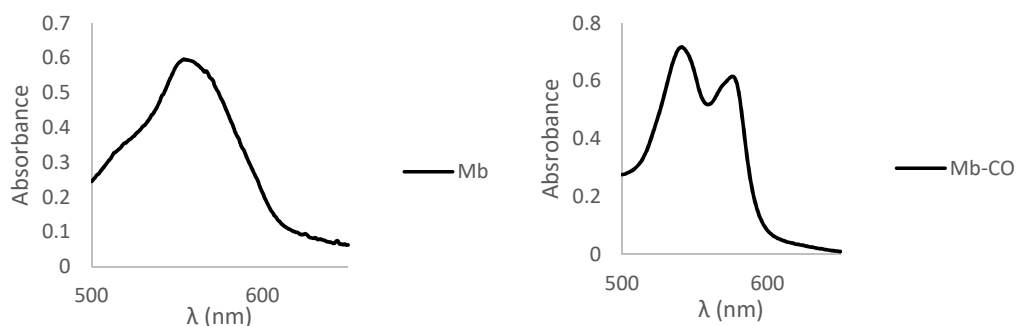


Figure 2.2 Absorbance spectra of Reduced myoglobin (Mb) and carbonmonoxy-myoglobin (Mb-CO).

2.5.2 Intracellular detection of CO released from CORMs

Carbon monoxide probe-1 (COP-1) is a fluorescent probe that is used to detect the presence of CO in solution or inside cells. This molecule contains a boron dipyrromethene difluoride (BODIPY), marked with a rectangle in Figure 2.1, which is a fluorescent probe that is quenched by palladium (Pd). When free CO inside cells reacts with COP-1, a carbonylation reaction occurs, releasing reduced Pd and fluorescent species (Figure 2.1)⁵⁹.

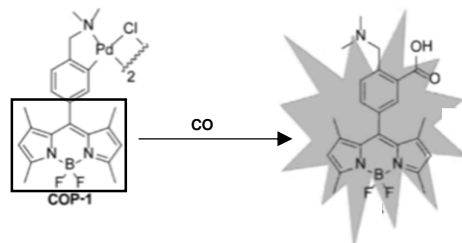


Figure 2.3 Carbonylation reaction of COP-1, with release of Pd. Adapted from Michel *et al.* (2012)⁵⁹.

For COP-1 assays, cell cultures with an OD_{600nm} of 0.1 were prepared from overnight grown cells and incubated at 37 °C, 150 rpm. When the cell suspensions reached an OD_{600nm} of 0.3, JM46 and JM47 were added to final concentrations of 8 μ g/ml to Gram-positive bacteria and 32 μ g/ml to Gram-negative bacteria. The cells were incubated for 15 minutes at 37 °C, 150 rpm. At

this stage COP-1 was added to a final concentration of 1 μM and the cells were once more incubated as previously described. Aliquots were prepared with a final OD of 5 in 333 μl (equation 2.1) and centrifuged for 10 minutes at 6000 rpm. All samples were washed with PBS (1 M). The resulting pellets were resuspended in 600 μl of PBS (1 M). Slides containing 900 μl of agarose (1.7 %) were prepared and 3 μl of the cell suspensions were added to each slide. All samples were analysed in the fluorescence microscope as described in section 2.4, with the FITC filter set. This experiment was repeated three times on *E. coli*, *S. enterica* and *S. aureus*, and each condition was tested in duplicate within each experiment.

2.6 Animal cell culture and toxicity assay

The porcine kidney epithelial cell line LLC-PK1, a widely utilised mammalian cell model, was used in the present work to evaluate the cytotoxicity of the CORMs under test. The cells were grown in Dulbecco's modified Eagle's medium (DMEM) supplemented with 10 % (v/v) heat-inactivated foetal bovine serum (FBS) and 1 % (v/v) of penicillin-streptomycin (Pen-Strep) mixture. Aliquots of the cell line were kept in DMEM supplemented with 20 % (v/v) FBS and 5 % (v/v) DMSO at $-80\text{ }^{\circ}\text{C}$ and in liquid nitrogen.

The viability of mammalian cells was determined by the half maximum inhibitory concentration (IC_{50}) using Thiazolyl Blue Tetrazolium Bromide (MTT). MTT is a positively charged compound that enters the cell. Once inside the mammalian cell mitochondria, the water soluble yellow tetrazolium salt MTT is reduced to formazan crystals. Formazan is a water-insoluble purple crystal that deposits at the bottom of the well and after being dissolved can be quantified spectrophotometrically at 550 nm. However, if a cell has no metabolic activity, the MTT will not be reduced into formazan crystals⁴¹. IC_{50} is then determined using as control healthy metabolically active cells. Tetrazolium salts have been used in 1942 to assess the germinating ability of seeds of different foods like corn, oats and wheat, based on the comparison in staining between seeds. These salts have been later utilised to assess the viability of different tissues⁶⁰. In 1983, Mosmann has demonstrated that the amount of MTT reduced to formazan is directly proportional to the number of viable cells in culture⁶¹. Since then, the MTT assay has been used to assess the cellular viability of several cell lines, under different conditions.

A frozen aliquot of LLC-PK1 cells was thawed for 1 to 2 minutes at $37\text{ }^{\circ}\text{C}$, transferred to a 15 mL sterile vial containing 10 mL of culture medium, centrifuged at 1100 rpm ($21\text{ }^{\circ}\text{C}$, for 5 minutes) and the supernatant was discarded. The pellet was resuspended in fresh medium, pre-heated at $37\text{ }^{\circ}\text{C}$, and transferred to a 25 cm^2 T-flask for incubation in an atmosphere containing 5 % CO_2 at $37\text{ }^{\circ}\text{C}$. Twenty-four hours later, the cells were analysed in the inverted microscope to verify the formation of the adherent monolayer and were sub-cultured afterwards. The cell line was

kept throughout the experiment by changing the media twice a week and when confluence reached 70-80 % cells were cultured into new 25 cm² T-flasks. To culture the cells into new T-flasks, the medium was removed, and the cells were washed with PBS (1 M). To promote the detachment of the monolayer from the flask, trypsin was added (2 mL) followed by incubation for 10 minutes at 37 °C. Inactivation of trypsin was achieved by addition of 4 ml of pre-heated culture medium. The cell suspension was divided in a 1:6 ratio and seeded into several new 25 cm² T-flasks containing fresh medium to achieve a final confluence of 30 %, in order to ensure a sufficient number of cells to perform the viability assays. Cells were incubated at 37 °C and 5 % CO₂. After 3 days of incubation, cells were first observed in the inverted microscope, to confirm their adherence and healthy state. The media was discarded, and the cells were washed with PBS (1M), and removed from the T-flask by addition of trypsin (2 mL) with 10 minutes of incubation at 37 °C. Cells were analysed in the inverted microscope to assess if all cells were in suspension. Fresh culture media was added (4 mL), and cells from all incubated T-flasks were collected into one vial and centrifuged at 1100 rpm, 21 °C, for 5 minutes. The supernatant was discarded and 10 ml of fresh medium was added. The cells were counted using the Trypan Blue staining method. Then, the cells were divided into 3 flasks, each containing 50000 cells/ml, and the content of each flask was then distributed into a 96 well-plate (200 µl in each well). The plates were incubated for 24 hours to allow cell seeding. On the second day, the compounds were administered to the cells, according to table 2.5. Three independent biological samples were tested in triplicate.

Table 2.5 Minimum and maximum concentrations of each compound administered to LLC-PK1 cells in the MTT assay.

Compounds	Range of concentrations tested (µg/mL)	
	Minimum	Maximum
JM46	0.25	8
JM47		
JM60	2	32
JM97		
JM107		
JM108		
JM109		
Clotrimazole		

After 24 hours of incubation at 37 °C in an atmosphere containing 5 % of CO₂, the culture medium was discarded and 100 µL of fresh medium containing 0.5 mg/mL of MTT, pre-heated at 37 °C, was added to each well. The cells were then incubated in the dark for 1 hour at 37 °C, in a 5 % CO₂ atmosphere. After removal of the MTT containing medium the formazan crystals deposited in the wells' bottom were solubilised by addition of 100 µl of DMSO. The absorbance was

measured spectrophotometrically at 550 nm. The same experiment was conducted after 48 and 72 hours of incubation. The IC_{50} was later calculated using the program GraphPad Prism 5, by fitting the best dose-response curve to the normalised data set.

3 Results

3.1 CORMs and ligands

In this study, 18 CORMs and 8 ligands were studied. These CORMs can be organised into 3 families according to the metal centre, as described in Table 3.1. The first family of CORMs is formed by ruthenium-containing compounds such as CORM-3, JM14, JM16 and JM94 with 3 CO groups, and JM106 with 2 CO groups. These compounds differ in the ligands bound to the metal centre. JM14 and JM106 have 2,2'-bipyridyl, JM16 has 1,10-phenanthroline and JM94 has a clotrimazole coordinated to the metal. The second family is composed by manganese centred CORMs and include HL2, JM20, JM32, JM42, JM46, JM60, JM62, JM69, JM80, JM97 and JM107. All manganese centred CORMs contain 3 CO groups, with the exception of JM60 and JM107 that contain 5 CO groups. The CORMs JM20, JM32, JM42, JM46 and JM97 have a 2,2'-bipyridyl ligand, JM80 has a 2,2'-bipyridyl-4,4'-dicarboxylic acid, JM60 contains a clotrimazole molecule, JM97 has the ligand JM108, JM107 has the ligand JM109, JM69 has a pyridine-2-carboxaldehyde, JM42 has a tris(hydroxymethyl)phosphine and lastly JM62 has a tetramethylethylenediamine. The third and final family is the smallest and is composed by rhenium centred CORMs such as JM20R, JM41 and JM47, all with 3 CO groups and a 2,2'-bipyridyl. JM47 has also a clotrimazole molecule and JM41 also a tris(hydroxymethyl)phosphine (Table 3.2).

The majority of the CORMs tested have manganese as the metal centre (Table 3.1). The most common ligand among all CORMs is 2,2'-bipyridyl, and the second one is clotrimazole (Table 3.2). Additionally, it is worth to notice that JM46 and JM47 are formed by JM20 and JM20R, respectively, plus a clotrimazole molecule that is coordinated to the metal centre.

Table 3.1 List of CORMs organised by metal-centre in alphabetical order.

Metal centre	CORMs										
Ruthenium	JM14	JM16	JM94	JM106							
Manganese	HL2	JM20	JM32	JM42	JM46	JM60	JM62	JM69	JM80	JM97	JM107
Rhenium	JM20R	JM41	JM47								

Table 3.2 List of CORMs organised by respective ligands in alphabetical order.

Ligands	CORMs
1,10-phenanthroline	JM16
2,2'-bipyridyl	JM14 JM20 JM20R JM32 JM41 JM42 JM46 JM47 JM106 JM97
2,2'-bipyridyl-4,4'-dicarboxylic acid¹	JM80
Clotrimazole	JM46 JM47 JM60 JM94
JM108	JM97
JM109	JM107
Pyridine-2-carboxaldehyde	JM32 JM69
Tetramethylethylenediamine	JM62
Tris(hydroxymethyl)phosphine	JM41 JM42

3.2 Determination of the Minimum Inhibitory Concentrations

The MIC assay was used to determine the bactericidal effect of the compounds under study. A range of concentrations, varying from 2 to 32 $\mu\text{g/ml}$ was tested for each compound, with the exception of JM46 and JM47, which tested concentrations ranged from 0.25 to 8 $\mu\text{g/ml}$. The MICs vary from 1 $\mu\text{g/ml}$ to more than 32 $\mu\text{g/ml}$, which was the highest concentration tested. For all the compounds tested, the MICs for *Escherichia coli* are above 32 $\mu\text{g/ml}$ and the MICs for *Staphylococcus aureus* and *Salmonella enterica* are presented in Table 3.3.

The compounds that have been further analysed (highlighted in bold in Table 3.3) were selected based on having MIC values below 32 $\mu\text{g/ml}$ or by being directly related to another compound that fulfils that criteria, as is the case of JM20 and JM20R, which are the precursors of JM46 and JM47, respectively. Furthermore, the compounds that share the same metal centre as CORM-3 were used for comparison purposes.

¹ The ligand 2,2'-bipyridyl-4,4'-dicarboxylic acid was not studied due to its low solubility.

JM20 and JM20R, the precursors of JM46 and JM47, respectively, are structurally similar differing only in the metal centre (Table 3.1). These CORMs present MICs higher than 32 µg/ml for *E. coli*, *S. enterica* and *S. aureus*. Furthermore, the clotrimazole ligand has a MIC of 16 µg/ml for *S. aureus* and higher than 32 µg/ml for *S. enterica* and *E. coli* (Table 3.3).

Table 3.3 Minimum Inhibitory Concentrations of the 26 compounds under study, for *Staphylococcus aureus* and *Salmonella enterica*, expressed in µg/ml.

Minimum inhibitory concentration (µg/ml)		
Compound	<i>S. enterica</i>	<i>S. aureus</i>
Clotrimazole	>32	16
JM46	>32	2
JM47	>32	1
JM60	>32	>32
JM97	8	32
JM108	4	16
JM109	4	8
1,10-Phenanthroline	16	>32
HL2, JM14, JM16, JM20, JM20R, JM32, JM41, JM42, JM62, JM69, JM80, JM94, JM106, JM107, Pyridine-2-carboxaldehyde, Tetramethylethylenediamine, Tris(hydroxymethyl)phosphine and 2,2'-bipyridyl	>32	>32

Compounds highlighted in **bold** have been selected for further analysis.

The compounds with strongest bactericidal activity are JM46 and JM47, which are structurally similar only differing in the metal centre (Table 3.1). As depicted in Table 3.3, JM46 and JM47 have MICs of 2 and 1 µg/ml for *S. aureus*, respectively, and higher than 32 µg/ml for *S. enterica* and *E. coli*. Therefore, these CORMs have increased activity when compared with the respective precursors, JM20 and JM20R, and when compared with the free ligand, clotrimazole.

The CORMs JM97 and JM107 are composed of a manganese metal centre conjugated to the organic ligands JM108 or JM109, respectively (Tables 3.1 and 3.2). The ligand JM108 exhibits a MIC of 16 µg/ml for *S. aureus* and 4 µg/ml for *S. enterica*. The MIC of JM97 was 32 µg/ml for *S. aureus* and *E. coli* and 8 µg/ml for *S. enterica*, therefore higher than those of the free ligand. For JM107, the bactericidal activity is also lower than that of its free ligand, JM109. The MIC of JM107 is higher than the maximum concentration tested, which is 32 µg/ml for all the bacteria under study, while its ligand has a MIC of 8 µg/ml for *S. aureus* and 4 µg/ml for *S. enterica*.

Complexes JM106, JM94, JM14 and JM16 are all ruthenium centred, like the vast majority of the CORMs so far studied (e.g. CORM-3), and for that reason are of great interest to study. Under the concentrations tested, all these compounds presented MIC values above 32 $\mu\text{g/ml}$ against all the tested bacteria. The 2,2'-bipyridyl ligand, which is coordinated to JM14 and JM106, also presented a MIC higher than 32 $\mu\text{g/ml}$ for all the strains. The coordination of 1,10-phenanthroline to JM16 somehow decreased the activity of the free ligand which presented a MIC of 16 $\mu\text{g/ml}$ for *S. enterica*. Finally, when comparing JM94 with the activity of its free ligand, clotrimazole, we observed a decrease in the bactericidal activity, since the complex presented a MIC higher than 32 $\mu\text{g/ml}$, while clotrimazole had a MIC of 16 $\mu\text{g/ml}$ for *S. aureus*.

3.3 Bacterial growth with CORMs

Growth curves were also obtained to evaluate the effects of the compounds on bacteria at different time points. The compounds were administered at equimolar concentrations in order to better compare the effects towards bacteria. The concentrations used were of 35 μM for *E. coli* and *S. enterica* and of 10 μM against *S. aureus*. These concentrations correspond to approximately 32 $\mu\text{g/ml}$ and 8 $\mu\text{g/ml}$ of JM47, respectively. The growth of untreated bacteria and treated with the solvent used to dissolve each compound were also analysed.

In *E. coli*, the exposure to 35 μM of the precursors of JM46 and JM47, JM20 and JM20R, did not affect bacterial growth. In fact, over the course of 24 hours, *E. coli* presented a survival rate of ~90 % or higher (Table S1). A similar behaviour is observed for clotrimazole, which is known to not eliminate Gram-negative bacteria³⁷. Although exposure of *E. coli* to 35 μM of JM47 does not kill the bacteria, when analysing the exposure hourly, a growth impairment with an apparent bacteriostatic effect was observed (Figure 3.1A). This CORM has effects immediately after 2 hours of exposure, slowing the growth of *E. coli* by half (Table 3.4). As for JM46, there was an impairment of *E. coli* growth over the first 2 to 3 hours after administration of 35 μM of CORM, and a survival rate of approximately 59 % after 3 hours. However, at later times the cells recovered and exhibited growth behaviour similarly to non-exposed cells, as the survival rate increased to 94 % after 4 hours of exposure (Figure 3.1B and Table 3.4).

Regarding the effects of the CORMs on *S. enterica* (Figures 3.2A and B), JM20 and JM20R presented no bactericidal effect over the course of 24 hours. Identically to what was observed for *E. coli*, in *S. enterica* an impairment of the growth was visible with 35 μM of JM46 in the first 2 to 3 hours after the treatment, with a survival rate of 73 %, followed by a strong recovery to reach OD values after 24 hours of incubation similar to non-treated cells (Figure 3.2A and Table S2). Additionally, *S. enterica* seems to also be affected by 35 μM of JM47, even though it presents a MIC higher than 32 $\mu\text{g/ml}$. The bacteriostatic effect was mainly visible in the first hours as the survival rate was maintained constantly low along the time (Figure 3.2B and Table S2). Although

clotrimazole did not seem to affect this Gram-negative bacterium by itself, it ameliorated the CORM activity, which is noticeable when comparing the growth curves of JM20R with JM47.

Both JM46 and JM47 impaired *S. aureus* growth immediately after the administration of 10 μ M, leading to an OD < 0.05 after 24 hours (Figures 3.3A and B), and a survival rate <10 % after just 2 hours of incubation (Table 3.3). This behaviour was neither observed when clotrimazole is absent from the molecular structure, as in the case of compounds JM20 and JM20R, nor when clotrimazole alone was used. Hence, when clotrimazole is coordinated to the CORM the bactericidal activity of the CORM increased. Clotrimazole is active against Gram-positive bacteria, so as expected, it affected bacterial growth of *S. aureus* but not as severely as JM46 and JM47 (Figure 3.3)³⁷. Clotrimazole presented a bacteriostatic effect in this bacterium as displayed in the growth curve. The cells presented a survival rate of 54 % after 2 hours of treatment, and of 40 % after 4 hours of treatment (Table 3.4). Furthermore, after 6 hours of treatment, the survival rate was 50 %, and after 24 hours was 47 %, demonstrating the bacteriostatic effect observed (Table S3).

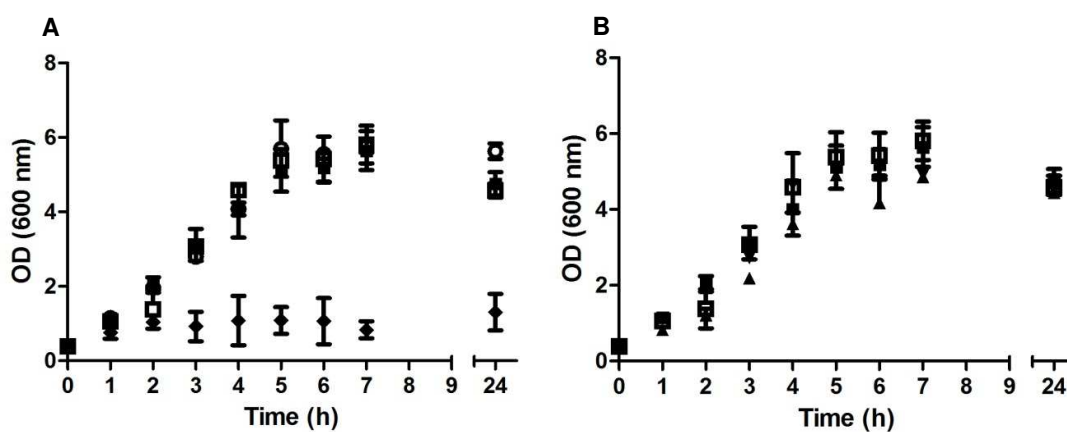


Figure 3.1 Growth curve of *E. coli* over 24 hours after treatment with 35 μ M of JM46, JM20, JM47, JM20Re, clotrimazole or 1 % DMSO, as control. (A) ■ Black square - DMSO; ◆ Black lozenge - JM47; ○ White Circle - JM20R; □ White square - clotrimazole. (B) ■ Black square - DMSO; □ White square - clotrimazole; ▲ Black Triangle - JM46; ▼ Inverted triangle - JM20.

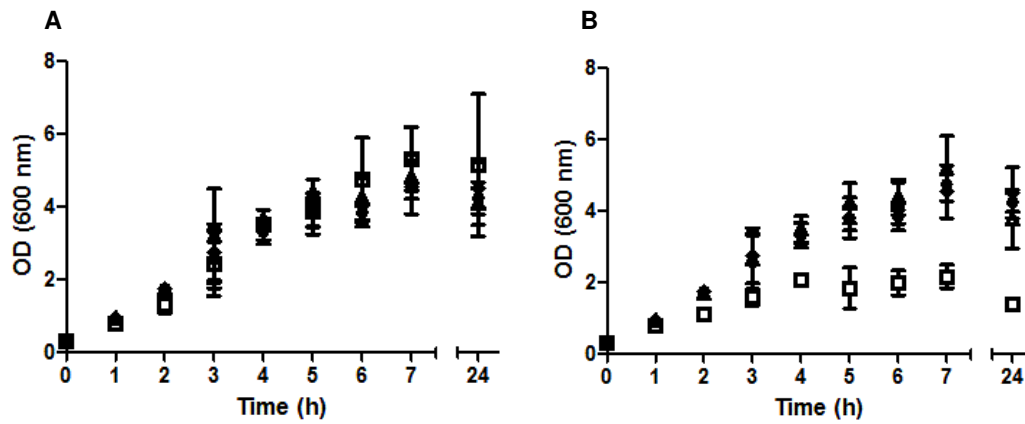


Figure 3.2 Growth curve of *S. enterica* over 24 hours after treatment with 35 μ M of JM46, JM20, JM47, JM20R, clotrimazole or 1 % DMSO, as control. (A) ● Black circle - DMSO; □ White square - JM46; △ White triangle - JM20; ◆ Black lozenge - clotrimazole. (B) ● Black circle - DMSO; □ White square - JM47; △ White triangle - JM20R; ◆ Black lozenge - clotrimazole.

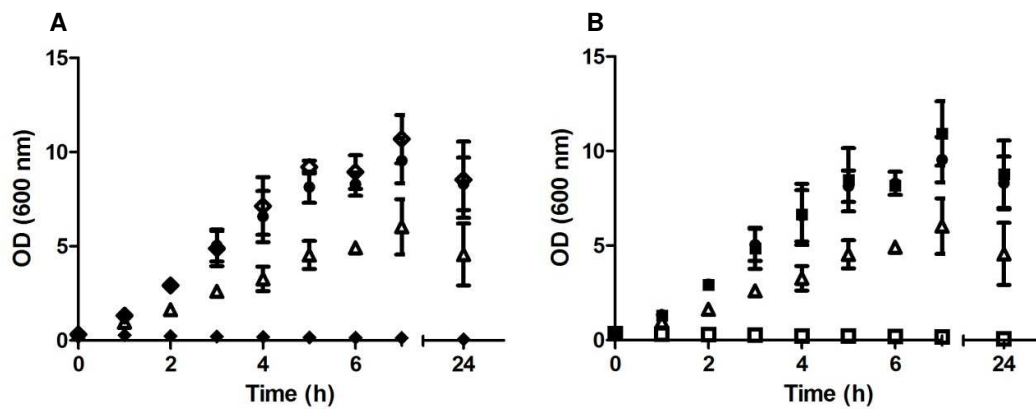


Figure 3.3 Growth curve of *S. aureus* over 24 hours after treatment with 10 μ M of JM46, JM20, JM47, JM20Re, clotrimazole or 1 % DMSO, as control. (A) ● Black circle - DMSO; ◆ Black lozenge - JM46; ◇ White lozenge - JM20; △ White triangle - clotrimazole. (B) ● Black circle - DMSO; □ White square - JM47; ■ Black square - JM20R; △ White triangle - clotrimazole.

Table 3.4 Percentage of survival of bacteria, upon treatment with JM46, JM20, JM47, JM20R and clotrimazole for 2 and 4 hours, at 35 μM for *E. coli* and *S. enterica* and 10 μM for *S. aureus*, and also upon treatment with 250 μM of CORM-3 for the three bacteria.

	Survival rate (%)					
	<i>E. coli</i>		<i>S. enterica</i>		<i>S. aureus</i>	
	2h	4h	2h	4h	2h	4h
JM46	59 \pm 2	94 \pm 8	73 \pm 12	105 \pm 6	8 \pm 1	2 \pm 1
JM20	90 \pm 6	119 \pm 16	97 \pm 1	110 \pm 10	99 \pm 6	96 \pm 10
JM47	46 \pm 9	28 \pm 11	62 \pm 8	63 \pm 2	9 \pm 1	3 \pm 1
JM20R	92 \pm 6	104 \pm 9	94 \pm 6	105 \pm 11	98 \pm 10	92 \pm 14
Clotrimazole	74 \pm 21	119 \pm 7	98 \pm 2	101 \pm 7	54 \pm 3	40 \pm 10
CORM-3	90 \pm 16	94 \pm 15	94 \pm 17	98 \pm 12	92 \pm 1	86 \pm 10

We were also interested in comparing the bactericidal effects of the new ruthenium-based CORMs, namely JM14, JM16, JM94 and JM106 with the widely studied CORM-3. Particularly how the different ligands used to coordinate to these new CORMs modulate their activity. In order to perceive significant differences, the concentration chosen was of 250 μM , half of the maximum bactericidal concentration of CORM-3². Therefore, all these complexes, including CORM-3, were tested at this concentration in the three bacterial strains and the cell growth was followed up to 4 hours. It was observed that after 2 hours of exposure to JM14 and JM16, both Gram-negative and Gram-positive bacteria suffered a significant growth impairment, specifically *S. aureus* (Figures 3.4A, 3.5A and 3.6A). On the other hand, JM94 and JM106 did not seem to affect the growth of Gram-negative bacteria, but JM94 caused a significant impairment of *S. aureus* after only 2 hours. After 4 hours of growth, *S. aureus* treated with JM14, JM16 and JM94, maintained the same OD values of the 2 hours exposure, indicating a bacteriostatic effect (Figure 3.4A). The same was observed for the Gram-negative bacteria exposed to JM14 and JM16. It was observed that JM94 treated cells after 4 hours continue to grow similarly to the non-treated cells (Figures 3.5A and 3.6A). Furthermore, JM106 did not impair the growth of any of the three bacteria even after 4 hours

² Nobre *et al.* have reported that CORM-3 presents a MIC of 400 μM to *E. coli* and 500 μM to *S. aureus*⁴⁶.

of exposure. When *S. aureus* was treated with JM106, it suffered a growth impairment similar to when it was treated with CORM-3 (Figure 3.4 A). However, when compared with JM14, JM16 and JM94, CORM-3 is significantly less active (Table 3.5).

The ligand of JM16, 1,10-phenanthroline, caused a significant growth impairment of all bacteria, particularly the Gram-negative bacteria *E. coli* and *S. enterica* (Figures 3.4 and 3.5). When comparing the results of the two Gram-negative bacteria, 1,10-phenanthroline impaired more the *E. coli* growth than that of *S. enterica* with a survival percentage of 19 and 26 upon 4 hours of treatment, respectively. On the other hand, JM16 was more active towards *S. aureus* than towards *E. coli* or *S. enterica*. Furthermore, for all the three organisms, this CORM has a higher activity when compared with its free ligand, 1,10-phenanthroline (Figures 3.4 to 3.6), presenting survival rates of 12 %, 12 % and 8 % against *E. coli*, *S. enterica* and *S. aureus*, respectively, after 4 hours of treatment (Table 3.4). The 2,2'-bipyridyl ligand, which is coordinated to JM14 and JM106, did not affect *S. aureus* growth, as this bacterium maintained a survival rate of 100 % throughout the experiment (Table 3.4). This ligand affected Gram-negative bacteria in a less severe manner than 1,10-phenanthroline as well, being the survival rate reduced to approximately half after 4 hours of treatment (Figures 3.4B, 3.5B and 3.6B). The CORM JM106 did not affect any of the bacteria under study, having lost the bactericidal activity of its ligand against Gram-negative bacteria. Moreover, JM14 presented a higher antimicrobial activity than its ligand against *E. coli*, *S. enterica* and *S. aureus* (Figures 3.4 to 3.6). Lastly, JM94 was only effective against *S. aureus* since its survival rate was 14 % upon 4 hours of treatment, which is very similar to its ligand, clotrimazole, which decreased the survival rate to 13 % in the same time frame (Figure 3.6 and Table 3.4).

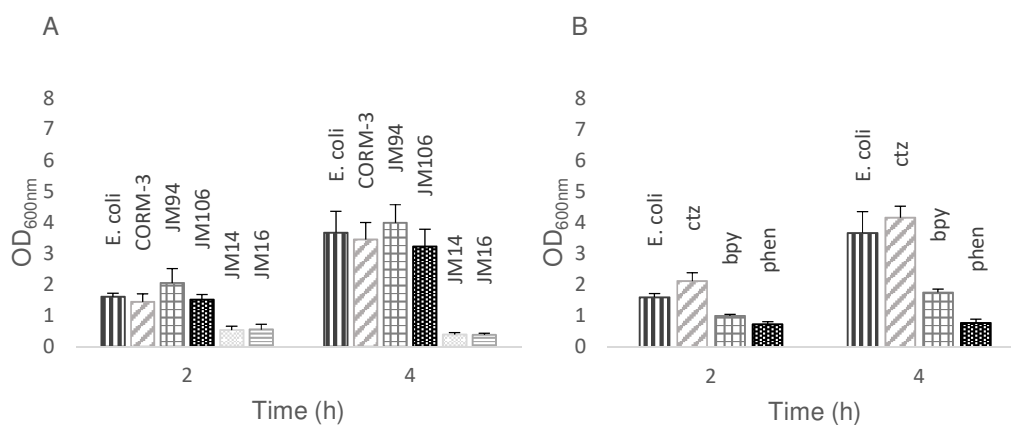


Figure 3.4 *Escherichia coli* growth inhibition 2 and 4 hours after exposure to 250 μ M of: **(A)** CORM-3, JM94, JM106, JM14 and JM16; and **(B)** ctz – clotrimazole; bpy – bipyridyl; phen – phenanthroline.

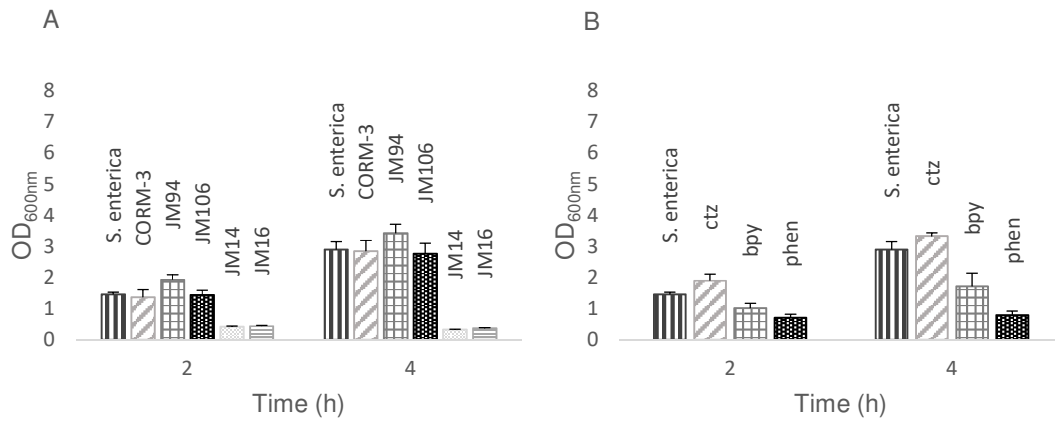


Figure 3.5 *Salmonella enterica* growth inhibition 2 and 4 hours after exposure to 250 μM of: **(A)** CORM-3, JM94, JM106, JM14 and JM16; and **(B)** ctz – clotrimazole; bpy – bipyridyl; phen – phenanthroline.

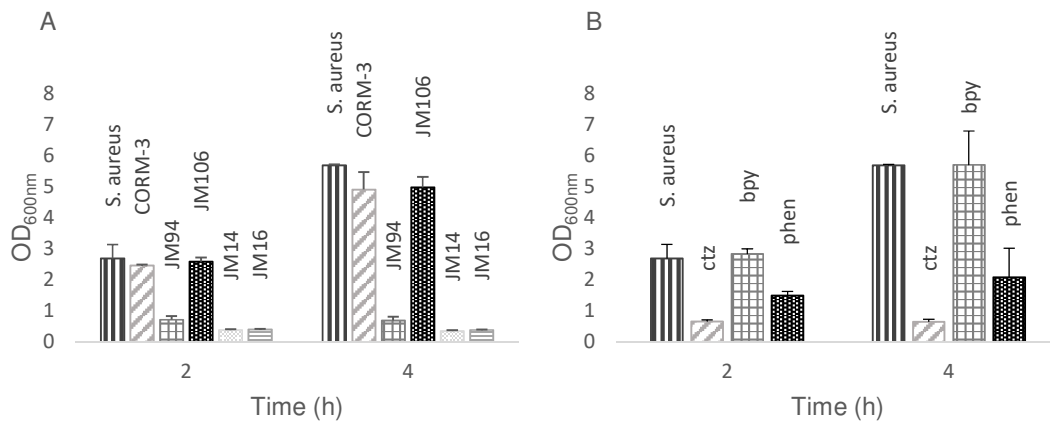


Figure 3.6 *Staphylococcus aureus* growth inhibition 2 and 4 hours after exposure to 250 μM of: **(A)** CORM-3, JM94, JM106, JM14 and JM16; and **(B)** ctz – clotrimazole; bpy – bipyridyl; phen – phenanthroline.

Table 3.5 Percentage of survival of *E. coli*, *S. enterica* and *S. aureus* upon administration of 250 μ M of the indicated CORMs and ligands.

	Survival (%)					
	<i>E. coli</i>		<i>S. enterica</i>		<i>S. aureus</i>	
	2h	4h	2h	4h	2h	4h
CORM-3	90 \pm 16	94 \pm 15	94 \pm 17	98 \pm 12	92 \pm 1	86 \pm 10
JM94	133 \pm 30	126 \pm 18	132 \pm 10	114 \pm 10	26 \pm 4	14 \pm 3
JM106	97 \pm 11	102 \pm 17	99 \pm 10	92 \pm 11	92 \pm 5	98 \pm 7
JM14	34 \pm 8	12 \pm 2	29 \pm 2	11 \pm 0.3	14 \pm 1	7 \pm 0.7
JM16	35 \pm 11	12 \pm 2	30 \pm 2	12 \pm 0.5	15 \pm 0.6	8 \pm 0.4
Clotrimazole	137 \pm 17	131 \pm 11	130 \pm 14	111 \pm 4	24 \pm 2	13 \pm 2
2,2'-bipyridyl	62 \pm 3	48 \pm 3	70 \pm 11	59 \pm 15	106 \pm 6	100 \pm 19
1,10-phenanthroline	42 \pm 5	19 \pm 3	43 \pm 7	26 \pm 4	50 \pm 4	38 \pm 17

3.4 Bacterial cell membrane permeability

To understand the mechanism of action sustaining the bactericidal effect of the CORMs analysed in this study, a staining assay that distinguishes live from dead bacterial cells was conducted. The LIVE/DEAD™ BacLight™ Bacterial Viability system allows the assessment of cell membrane permeability. This assay involves two bacterial stains, SYTO™ 9 and propidium iodide, the first enters all cells, dead or alive, and the second stain is only able to penetrate cells with a compromised membrane, which are considered dead. Bacterial cells with compromised cellular membranes become fluorescent yellow-red, whereas healthy bacteria with intact membranes are fluorescent green. The protocol was performed 2 and 24 hours after incubation of the cells with the compounds JM46 and JM47, which are the most active of all CORMs tested. Microscope images of the CORM-treated cells were acquired and compared with the DMSO treated cells, the solvent of JM46 and JM47.

For *E. coli*, exposure to JM46 and JM47 (32 μ g/ml) for 2 hours resulted in approximately 50 % of non-viable cells as shown by the noticeable decrease in cell density. Furthermore, these bacteria presented an elongated shape as can be observed in the microscope images (Figures 3.7A and B). These results are coherent with what was previously observed in the growth curves (Figure 3.1). After 24 hours, cells exposed to JM46 recovered cell density and their morphology (Figure 3.7D). Also, the proportion of non-viable cells, which appear yellow-red, was similar to that of the control cells that were treated with the same amount of DMSO present in the CORM solution

(Figures 3.7D and F). After exposure to JM47 for 24 hours, *E. coli* maintained the low cellular density and retained the abnormal elongated morphology (Figure 3.7E).

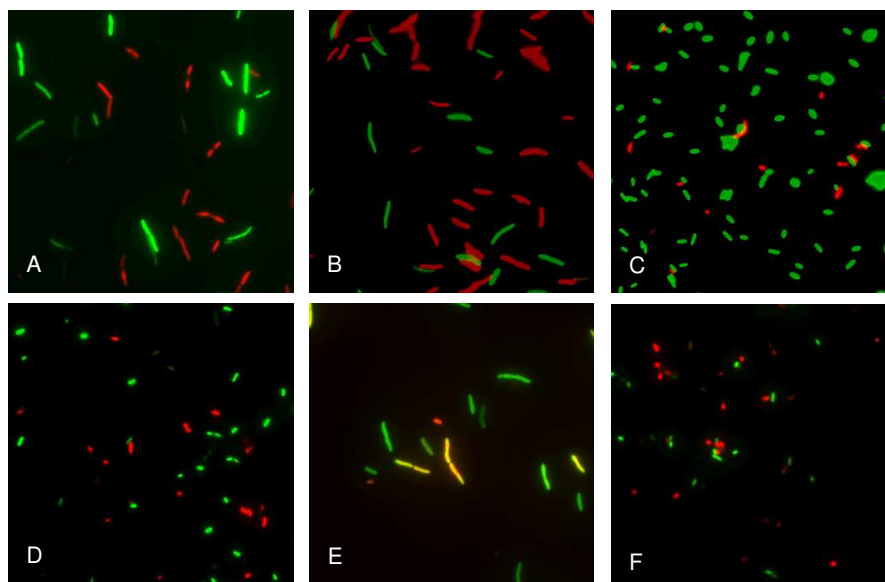


Figure 3.7 *E. coli* cell membrane permeability upon treatment with CORMs. Microscope images of the effect of JM46 and JM47 after 2 and 24 hours of incubation, evaluated by the Live/Dead viability staining method. Live and healthy bacteria with intact membrane are stained green (SYTO9), and dead bacteria or unhealthy with damaged membranes are stained yellow-red (propidium iodide). **(A)** JM46 at 32 $\mu\text{g}/\text{ml}$, 2 hours after exposure; **(B)** JM47 at 32 $\mu\text{g}/\text{ml}$, 2 hours after exposure; **(C)** DMSO at 1 %, 2 hours after exposure; **(D)** JM46 at 32 $\mu\text{g}/\text{ml}$, 24 hours after exposure; **(E)** JM47 at 32 $\mu\text{g}/\text{ml}$, 24 hours after exposure; **(F)** DMSO at 1 %, 24 hours after exposure.

Salmonella enterica exposed to JM46 and JM47 (32 µg/ml, for 2 hours) presented a reduction in cellular density, which was less accentuated when exposed to JM46 than to JM47. Furthermore, when exposed to JM46 or JM47 (2 hours) the proportion of cells with increased membrane permeability or non-viable was higher in comparison with cells exposed to DMSO, which is the control (Figures 3.8A, B and C). Also, there was still a significant decline in cell density, for the population exposed to JM47 for 24 hours and the same proportion of non-viable cells as in the population exposed for 2 hours (Figures 3.8B and E). On the contrary, after 24 hours of exposure to JM46 *S. enterica* showed recovery in cellular viability and in cellular density in comparison with the cells exposed to DMSO (Figures 3.8D and F). For both *S. enterica* cells exposed to JM46 and JM47 (2 hours), it is also possible to observe their elongated shape, similar to what was observed for *E. coli*, yet less evident (Figures 3.8A and B). However, the population of *S. enterica* under JM46 effects during 24 hours of exposure, recovered its normal morphology. The cells exposed to JM47 did not show this recovery, again similarly to what was observed in *E. coli*.

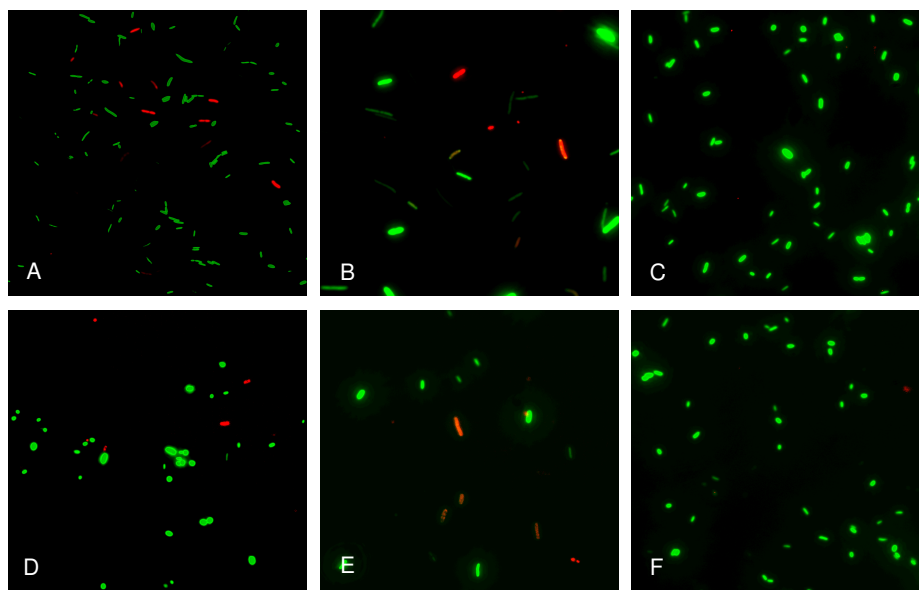


Figure 3.8 *S. enterica* cell membrane permeability upon treatment with CORMs. Microscope images of the effect of JM46 and JM47 after 2 and 24 hours of incubation, evaluated by the Live/Dead viability staining method. Live and healthy bacteria with intact membrane are stained green (SYTO9), and dead bacteria or unhealthy with damaged membranes are stained yellow-red (propidium iodide). (A) JM46 at 32 µg/ml, 2 hours after exposure; (B) JM47 at 32 µg/ml, 2 hours after exposure; (C) DMSO at 1 %, 2 hours after exposure; (D) JM46 at 32 µg/ml, 24 hours after exposure; (E) JM47 at 32 µg/ml, 24 hours after exposure; (F) DMSO at 1 %, 24 hours after exposure.

S. aureus exposed to JM46 and JM47 (8 µg/ml, for 2 hours) presented a significant increase in membrane permeability, with the vast majority of the cell population coloured yellow-red

in comparison with cells exposed to DMSO (1 %). This effect is more accentuated after 24 hours of exposure.

From the 3 organisms studied, *S. aureus* is the one in which the effect of the compounds on the membrane permeability is more significant, particularly for JM47, which is in agreement with the growth inhibition previously shown (Figures 3.3 and 3.9). For *S. aureus* cells exposed to JM46 and JM47 there is a significant decrease in cellular density. In order to obtain the same final cellular density in the microscope slide higher volumes of treated bacterial cultures were recovered in comparison with untreated bacterial cultures

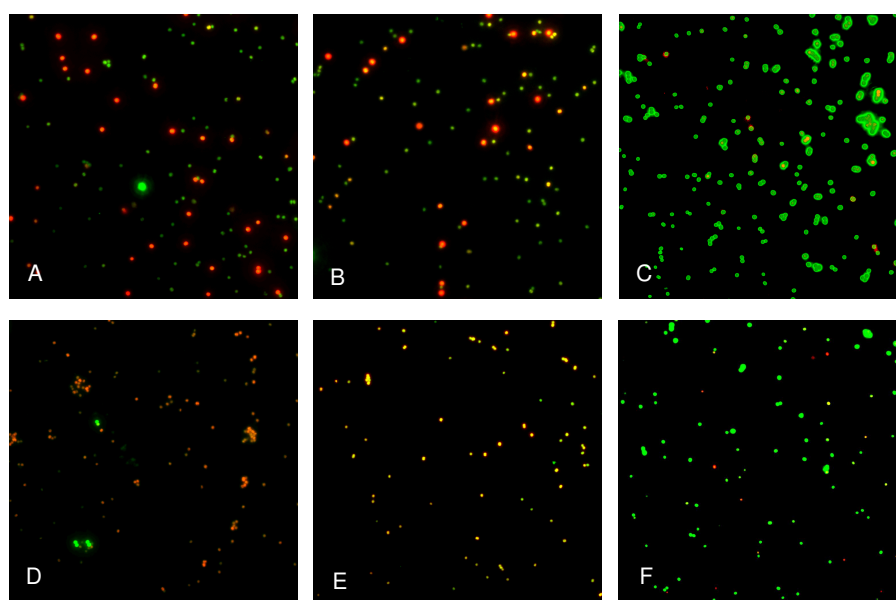


Figure 3.9 *S. aureus* cell membrane permeability upon treatment with CORMs. Microscope images of the effect of JM46 and JM47 after 2 and 24 hours of incubation, evaluated by the Live/Dead viability staining method. Live and healthy bacteria with intact membrane are stained green (SYTO9), and dead bacteria or unhealthy with damaged membranes are stained yellow-red (propidium iodide). (A) JM46 at 8 $\mu\text{g/ml}$, 2 hours after exposure; (B) JM47 at 8 $\mu\text{g/ml}$, 2 hours after exposure; (C) DMSO at 1 %, 2 hours after exposure; (D) JM46 at 8 $\mu\text{g/ml}$, 24 hours after exposure; (E) JM47 at 8 $\mu\text{g/ml}$, 24 hours after exposure; (F) DMSO at 1 %, 24 hours after exposure.

3.5 Myoglobin assay

The CO release by JM46, JM47, JM20 and JM20R was assessed spectrophotometrically, in the presence of a CO scavenger, myoglobin and under anaerobic conditions. In these experiments, the compounds were dissolved and rapidly added to myoglobin (1:1, 60 μM) previously reduced with sodium dithionite in PBS (0.1 M). This mixture was transferred to a purged quartz cuvette, and a first spectrum was taken immediately. Spectra were acquired every 30 minutes up to 2 hours. The CO release was observed by tracking the conversion of reduced myoglobin to carbonmonoxy-

myoglobin (Mb-CO). The reduced myoglobin spectrum exhibits a single absorbance peak at 555 nm, while Mb-CO displays two absorbance peaks at 540 nm and 570 nm (Figure 3.10).

Immediately after the addition of JM46 to the myoglobin solution (time zero) no major change in the Mb spectrum at 550 nm was observable. The formation of the Mb-CO characteristic spectrum was observable after 60 minutes of incubation of JM46 with the reduced myoglobin. These two peaks at 540 and 570 nm become better defined after 90 minutes of incubation (Figure 3.11).

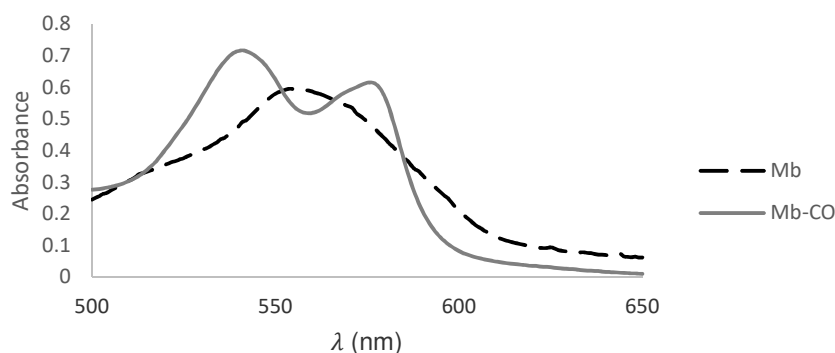


Figure 3.10 Absorbance spectra of myoglobin (Mb) represented by the dashed black line, and carbonmonoxy-myoglobin (Mb-CO) represented by the full grey line.

For JM20, the formation of Mb-CO is detected 30 minutes after addition of the CORM to the reduced myoglobin. Along the time, up to 120 minutes, these peaks become more defined, suggesting a gradual and continuous release of CO (Figure 3.11). After 120 minutes of incubation with this CORM there is a release of 6.9 μM of CO from the molecule (Table 3.6). The precursor JM20 liberates 6.9 μM of CO after 2 hours of incubation, whereas JM46 liberates 17 μM in the same period of time, *i.e.* the concentration of Mb-CO formed is 2.5 times higher for JM46 (Table 3.6) This indicates that the addition of clotrimazole to the molecular structure of the CORM contributed to the lability of the CO molecules present.

For JM47, the formation of Mb-CO is observed after 60 minutes of incubation, and kept increasing till the 120 minutes of reaction, similarly to what was observed for JM46 (Figure 3.11). However, the concentration of Mb-CO formed is significantly lower than the concentration formed in the case of JM46. This CORM appears to be of higher stability than JM46, liberating short amounts of CO molecules throughout the time (Table 3.6).

In the case of JM20R, the Mb spectrum remains unaltered during the 120 minutes of incubation (Figure 3.11). This indicates that no Mb-CO is being formed over time and that this

CORM does not release CO spontaneously and is stable in PBS (Table 3.6). Furthermore, the coordination of clotrimazole to JM20R results in an increase of the CO release from the CORM.

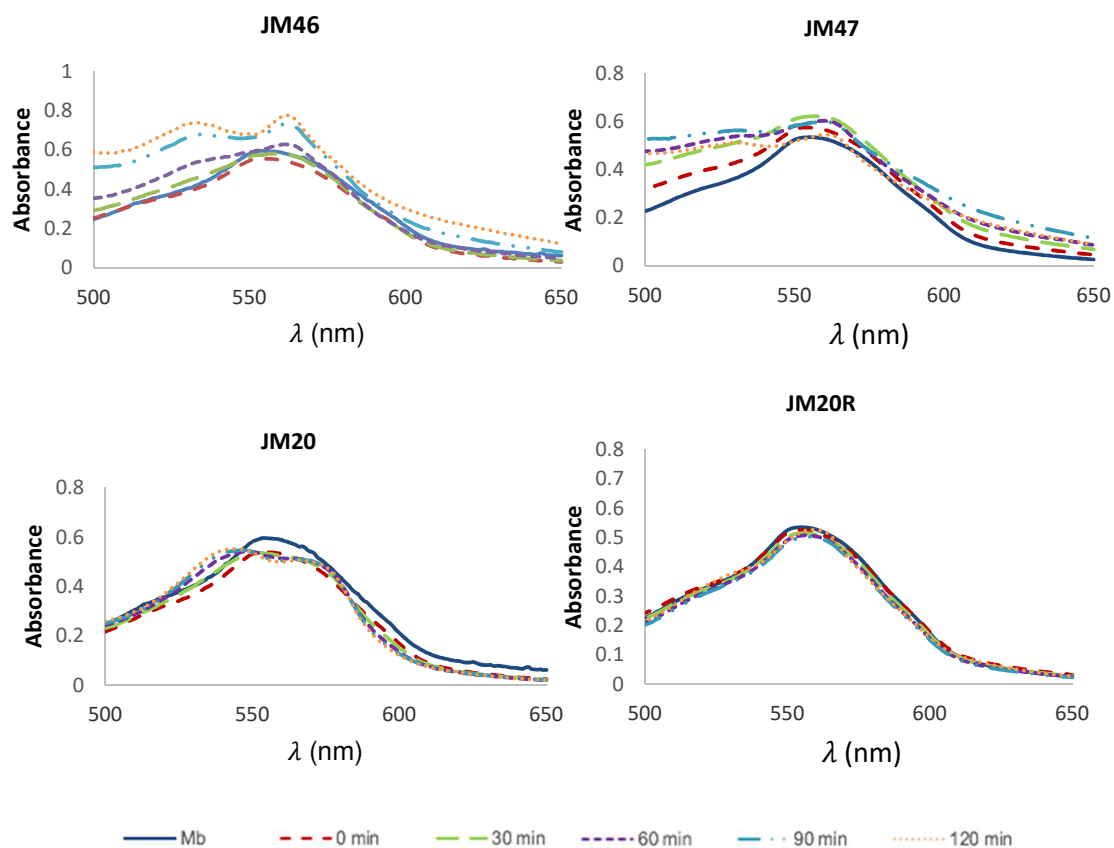


Figure 3.11 Absorbance spectra of myoglobin (Mb) in the presence of JM46, JM47, JM20 and JM20R for 120 minutes. Spectra were obtained at 0 minutes (burgundy), 30 minutes (green), 60 minutes (purple), 90 minutes (blue) and 120 minutes (orange).

Table 3.6 Carbonmonoxy-myoglobin (Mb-CO) formed, throughout the time of incubation of Mb with the complexes JM46, JM20, JM47 and JM20R, expressed in μM .

Time (min)	Mb-CO (μM)			
	JM46	JM20	JM47	JM20R
0	0.0	0.0	0.0	0.0
30	3.0	2.6	4.0	0.0
60	6.9	5.0	3.9	0.0
90	14.2	6.1	4.7	0.0
120	17.0	6.9	0.9	0.0

3.6 Intracellular detection of CO released from CORMs

In order to assess the intracellular release of CO by JM46 and JM47 inside bacteria, the fluorescent carbon monoxide probe 1 (COP-1) was used. This probe enters the bacterial cells and binds the free intracellular CO, generating fluorescent green cells that were observed by microscopy. In all cases, the cells were incubated for 15 minutes with the CORMs before addition of the COP-1.

When COP-1 was incubated with cells from all the three bacteria strains under study treated with 1 % of DMSO, no fluorescence was observed, as expected (Figure 3.12), since there was no free CO available to bind to the probe, meaning that the BODIPY fluorescence was still being quenched by Pd.

Escherichia coli cells exposed to JM46 or JM47 (8 $\mu\text{g}/\text{mL}$) exhibited approximately half of its population fluorescent. Furthermore, localised fluorescence across the cells and differences in fluorescence intensity across the population is evident for both JM46 and JM47, indicating that the distribution of the CORMs is not homogenous throughout the population (Figure 3.13).

Salmonella enterica exposed to JM46 and JM47 (8 $\mu\text{g}/\text{mL}$), exhibited lower percentage of fluorescent cells when compared to *E. coli*. Even though only a few cells are fluorescent, there was not a difference in fluorescence throughout the population as observed for *E. coli*. It was also not visible an accentuated localised fluorescence inside the cells as seen in *E. coli*, which indicates that JM46 and JM47 release CO more homogeneously inside *S. enterica* (Figure 3.13).

Staphylococcus aureus cells pre-exposed to 8 µg/ml of JM46 or JM47 and incubated with COP-1 exhibit a homogeneous bacterial population fluorescence. Moreover, no major difference is observed in cells exposed to JM46 or to JM47. From all three organisms, these bacterial cells were the only ones that exhibited fluorescence equally throughout all population and without localised intracellular fluorescence (Figure 3.13).

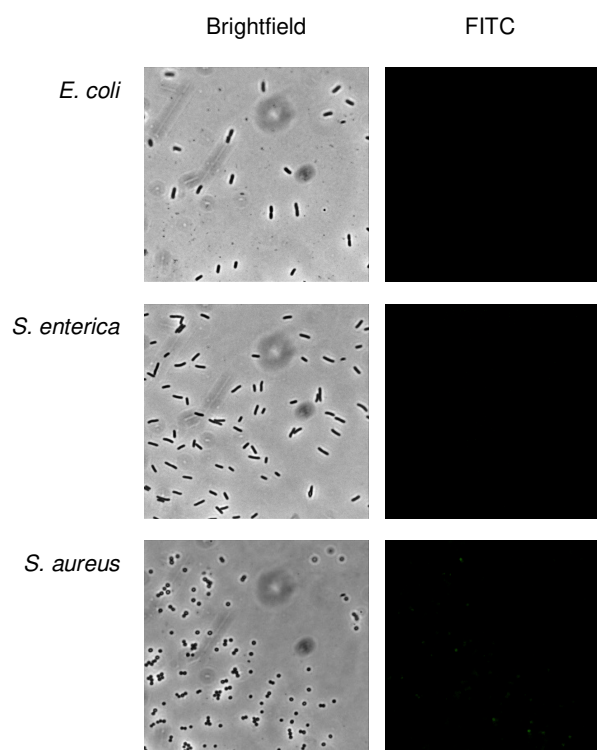


Figure 3.12 Detection of CO release intracellularly utilizing a fluorescent probe, COP-1. Microscope images of three organisms: *E. coli* (first row), *S. enterica* (second row) and *S. aureus* (third row), after exposure to DMSO (1 %). For each organism there is a microscopy image (Brightfield) and the corresponding fluorescent image (FITC).

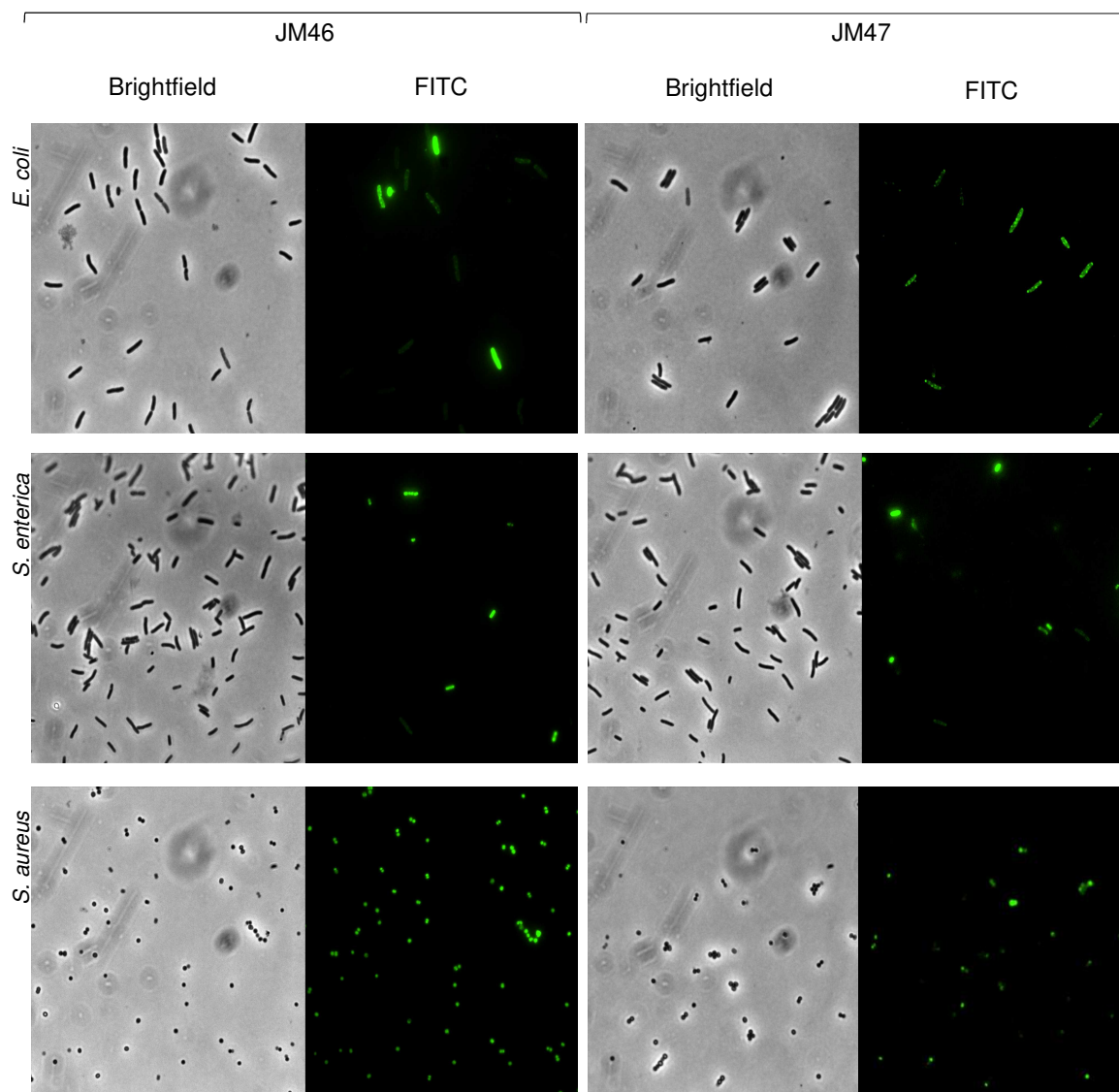


Figure 3.13 Detection of CO release intracellularly utilizing a fluorescent probe, COP-1. Microscope images of three organisms: *E. coli* (first row), *S. enterica* (second row) and *S. aureus* (third row), after exposure to two CORMs: JM46 (left column) and JM47 (right column). Each column presents a microscopy image (Brightfield) and the corresponding fluorescent image (FITC).

3.7 Animal cell toxicity assays

Another important parameter to be analysed is the cytotoxicity of the CORMs towards mammalian cells. The cytotoxicity was assessed by measuring the cell viability using the MTT assay. The results are expressed as percentages of viability relatively to untreated cells and also by the half maximum inhibitory concentration values, IC_{50} , for each endpoint. The LLC-PK1 porcine kidney cell line, a widely utilised mammalian cell model, was used for this experiment. The compounds JM46 and JM47 were added to the cells in concentrations ranging from 0.25 to 8 $\mu\text{g/ml}$ and the compounds JM60, JM97, JM107, JM108, JM109 and clotrimazole were added to the cells in concentrations ranging from 2 to 32 $\mu\text{g/ml}$. The cells were incubated for 24, 48 or 72 hours, at 37 $^{\circ}\text{C}$ in an atmosphere containing 5 % of CO_2 . The cell viability and the IC_{50} were determined as described in the materials and methods section.

Clotrimazole, which is present in the JM46 and JM47 molecules, shows cytotoxicity with an IC_{50} of 8.9 $\mu\text{g/ml}$ after incubation for 24 hours, which decreases to 5.4 $\mu\text{g/ml}$ after 72 hours of exposure (Table 3.7). The cells show less viability with the increase of time exposure to the drug, for all the concentrations tested (Figure 3.14H). The coordination of clotrimazole to the metals manganese (JM46) and rhenium (JM47) enhances the ligand's cytotoxicity, as the IC_{50} of these two CORMs is less than half of the IC_{50} of the ligand (Table 3.7).

The results show that JM46 and JM47 have an IC_{50} average of approximately 2.1 and 2.5 $\mu\text{g/ml}$, respectively (Table 3.7). These IC_{50} are in the same order of magnitude of the MIC values of these compounds (2 and 1 $\mu\text{g/ml}$ respectively, for *S. aureus*) therefore, these are cytotoxic to eukaryotic cells. Over time (24, 48 and 72 hours), CORMs cytotoxicity was not altered as the IC_{50} remained similar throughout the three days of incubation (Table 3.7). For both JM46 and JM47, the cell viability is less than 50 % after treatment with 4 $\mu\text{g/ml}$ and close to 0 % when treated with 8 $\mu\text{g/ml}$, indicating the high cytotoxicity of these CORMs (Figures 3.14A and B).

JM60 is a little more toxic over time, as for cells incubated for 24 hours have an IC_{50} of 23.6 $\mu\text{g/ml}$, and cells incubated for 48 and 72 hours have an IC_{50} of approximately 20.5 $\mu\text{g/ml}$ (Table 3.7). The time factor influences cellular viability for concentrations of 8 $\mu\text{g/ml}$ or under, as in these conditions this CORM becomes more toxic at 72 hours. However, for concentrations of 16 $\mu\text{g/ml}$ or above, the incubation time does not seem to influence the cytotoxic effect, as there were no significant differences between cells incubated for 24 or 72 hours (Figure 3.14 C).

Furthermore, the cytotoxicity of JM108 and JM109, the ligands of JM97 and JM107, respectively, was analysed (Figures 3.14F and G). JM108 and JM109 lost their cytotoxicity at 72 hours of incubation for all concentrations tested, indicating a limited time effect. Furthermore, at 24 hours of incubation, JM108 (IC_{50} of 28 $\mu\text{g/ml}$) was more cytotoxic than JM109 (IC_{50} above 32 $\mu\text{g/ml}$) (Table 3.7).

Compounds JM97 and JM107 have IC_{50} values higher than 32 $\mu\text{g/ml}$, which was the maximum concentration tested (Table 3.7). For both JM97 and JM107, at the incubation time of 72 hours and for any of the concentrations tested there was no cytotoxic effect observed, with the exception of a small decrease in cell viability when 32 $\mu\text{g/ml}$ of JM97 were used. Additionally, the cells appear to become more viable with the increase of the incubation time, as the compounds lose their cytotoxic properties (Figures 3.14D and E). These results indicate that like their ligands, these CORMs have a limited time effect for the first 24 hours of treatment. Additionally, similarly to what was observed against bacterial cells, JM108 toxicity is lost when coordinated to the metal.

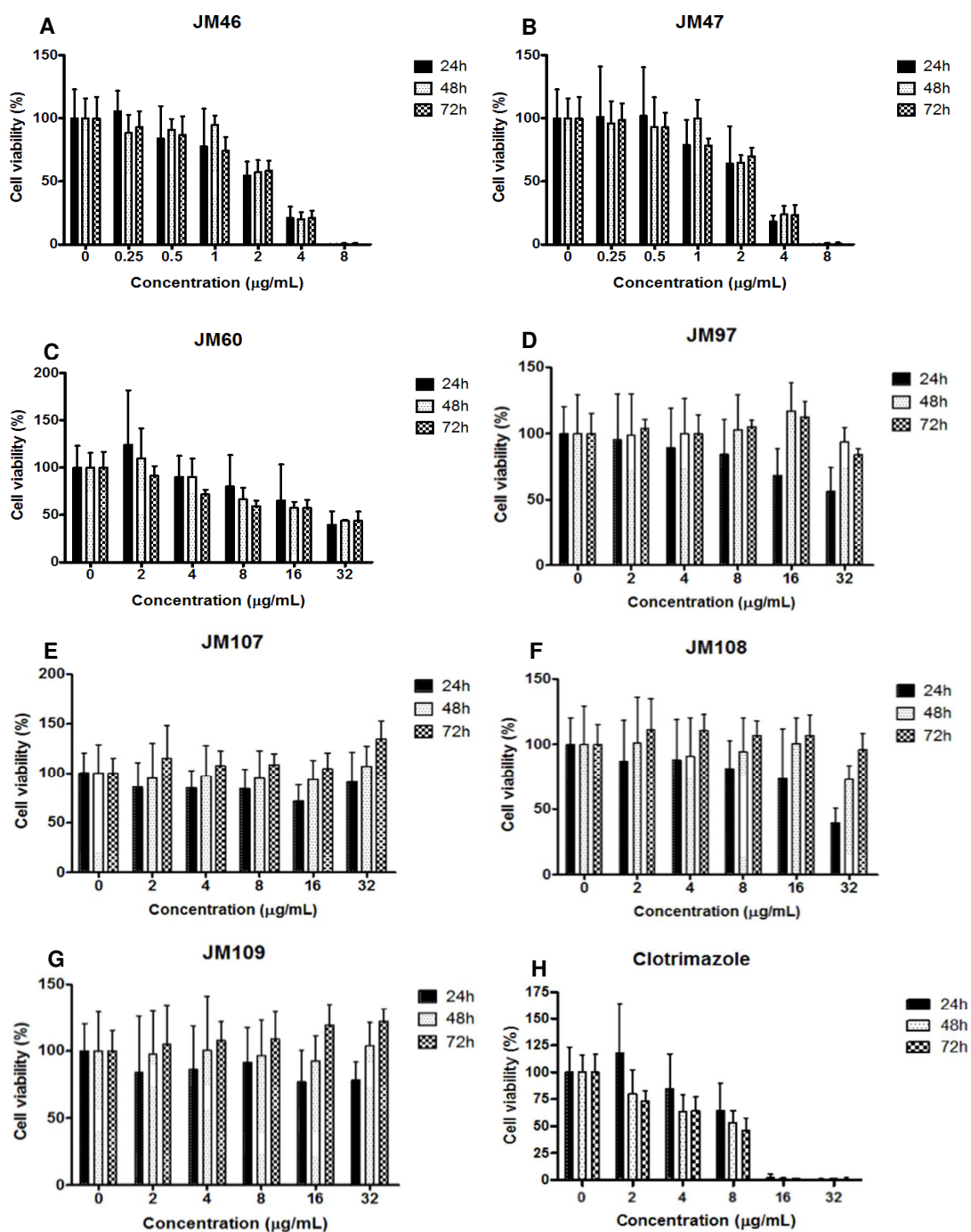


Figure 3.14 Cytotoxicity of CORMs and ligands was evaluated in LLC-PK1, using (A) JM46, (B) JM47, (C) JM60, (D) JM97, (E) JM107, (F) JM108, (G) JM109 and (H) clotrimazole. With the exception of JM46 and JM47, whose concentrations ranged from 0.25 to 8 µg/ml, all CORMs were tested with concentrations going from 2 to 32 µg/ml. Individual columns in each graph represent the period of incubation: 24, 48 and 72 hours. Cell viability was determined relatively to untreated cells.

Table 3.7 Half maximum inhibitory concentration of the compounds against LLC-PK1, after incubation for 24, 48 and 72 hours, expressed in $\mu\text{g/ml}$.

Compounds	IC ₅₀ ($\mu\text{g/mL}$)		
	24 hours	48 hours	72 hours
JM46	2.0	2.3	2.0
JM47	2.3	2.6	2.5
JM60	23.6	20.5	20.7
JM97	>>32	>>32	>>32
JM107	>>32	>>32	>>32
JM108	28.0	25.1	25.0
JM109	>>32	>>32	>>32
Clotrimazole	8.9	6.0	5.4

4 Discussion

According to the WHO, the strains studied in this work, namely *Escherichia coli*, *Staphylococcus aureus* and *Salmonella* spp. are among the most common antibiotic resistant bacteria. These pathogens infect debilitated people through several disease spreading vehicles, and are usually hospital acquired infections (HAIs)²⁷. Additionally, WHO has reported that 4 to 56 % of neonatal deaths in hospitals are a consequence of HAIs, and that worldwide 1 in 10 patients are infected by HAIs⁶². The emergence of these life-threatening antimicrobial-resistant bacteria requires the development of new types of antibiotics.

For many years, transition metals have been employed as drugs to treat several diseases. For example, the metal containing silver sulfadiazine is commonly used as a topical antimicrobial in patients with burns, and in catheters to prevent infections as it is effective in avoiding the propagation of bacteria^{63,64}. Also, radioactive ruthenium is often used in cancer treatment. More recently, metal CORMs including ruthenium CORMs have been considered potential drugs for medical purposes⁶⁵. In particular, CORMs have demonstrated to have bactericidal activity, apparently with low associated cytotoxicity to mammalian cells^{41,46}.

In this work we addressed the study of CORMs that may be of use to fight infections by testing 18 new CORMs (and 8 ligands) having shown that 2 of them, namely JM46 and JM47 are very active against the Gram-positive bacterium *S. aureus*. These CORMs have MICs of 2.5 and 1 μM , respectively, that are significantly more bactericidal than another family of CORMs previously analysed against *S. aureus*, which included ALF021, ALF062, CORM-2 and CORM-3 (Table 4.1)⁴⁶. However, none of the 26 compounds tested in this work presented bactericidal effects against *E. coli* at concentrations below 32 $\mu\text{g/ml}$ (Table 3.2), but some of these compounds, such as JM97, JM108 and JM109, were bactericidal against *S. enterica*. Interestingly, these compounds were more active against *S. enterica* than to *S. aureus*.

Table 4.1 Concentrations of CORMs that kill *E. coli* and *S. aureus* under aerobic conditions, from Nobre *et al.* (2007)⁴⁶.

CORM	Concentration (μM)	
	<i>E. coli</i>	<i>S. aureus</i>
ALF021	500	600
ALF062	50	50
CORM-2	250	250
CORM-3	400	500

These results showed that among the three organisms tested *S. aureus* was, in general, the bacterium more sensitive to CORMs. Indeed, for *S. aureus*, six CORMs presented MIC values under 32 $\mu\text{g/ml}$, whereas for *S. enterica* only four compounds had MIC values under 32 $\mu\text{g/ml}$.

Earlier studies also showed that CORM-2, CORM-3 and the ALF family of CORMs were more active towards Gram-negative⁴⁶.

Altogether, these results suggest that, in contrast with other small molecules, the outer membrane of the Gram-negative bacteria is not easily permeable to CORMs. Furthermore, the higher efficacy against *S. aureus* may be due to the absence of an outer membrane.

Although in itself ruthenium seems to be relatively inert, some ruthenium complexes are known to bind to DNA and proteins, and to show antimicrobial effects⁶⁵. Two ruthenium complexes were reported by Li *et al.* to be highly toxic for *P. aeruginosa* and especially to *E. coli* and MRSA, with MICs of 2 and 1 µg/ml, respectively⁶⁶. Furthermore, Bolhuis *et al.* synthesised ruthenium complexes with coordinated ligands^c, namely [Ru(phen)₂(dpq)]²⁺, [Ru(bpy)₂(dpqC)]²⁺, and [Ru(2,9-Me₂phen)₂(dppz)]²⁺, that presented significant bactericidal activity against Gram-positive bacteria, but not to Gram-negative bacteria. These complexes bind to and intercalate with DNA, with some of them exhibiting a MIC against MRSA as low as 2 µg/ml⁶⁷. In 2007, the ruthenium centred CORM-2 and CORM-3 were also reported as bactericidal agents against Gram-positive and Gram-negative bacteria, even though at higher concentrations (Table 4.1)⁴⁶.

In this work, we wanted to assess if the new ruthenium-centred CORMs were more active than CORM-2 and CORM-3. The novel synthesised ruthenium centred CORMs JM14, JM16, JM94 and JM106 presented MICs higher than 32 µg/ml for Gram-positive and Gram-negative bacteria. To compare these ruthenium CORMs with CORM-3, they were tested at a concentration of 250 µM, which is lower than the MIC of CORM-3. Data showed that JM14, JM16 and JM94 are more toxic than CORM-3. *S. aureus* treated with JM94 for 2 hours presented a decrease of 75 % in survival when compared to untreated cells, while *S. aureus* treated with CORM-3 suffered a survival decrease of only 9 %. The decrease is even more significant after 4 hours of treatment, being ~86 % for JM94 and ~14 % for CORM-3. Interestingly, CORM-3 is more toxic to *E. coli* than to *S. aureus* (Table 4.1), which did not occur with the other ruthenium CORMs that were tested in this work, JM14, JM16 and JM94 (Table 3.2)⁴⁶.

Of the 5 ruthenium CORMs tested, the most active one was JM14 with survival rates of 12 % for *E. coli*, 11 % for *S. enterica* and 7 % for *S. aureus*. Additionally, this CORM is about 2 times and 1.5 times more toxic than CORM-3 against *S. aureus* and *E. coli*, respectively. Furthermore, JM14 has a similar toxicity as CORM-2, which presents MICs of 250 µM for both *E. coli* and *S. aureus* (Table 4.1).

^c The ligands that the authors used in the metal complexes were: dipyrido[3,2-d:2',3'-f]quinoxaline (dpq); dipyrido[3,2-a:2',3'-c](6,7,8,9-tetrahydro) phenazine (dpqC); and dipyrido[3,2-a:2',3'-c]phenazine (dppz).

JM16 is also very toxic to bacteria. *E. coli* and *S. enterica* exposed to JM16 have a survival rate of 12 % and *S. aureus* of 8 %. Hence, this CORM has an efficacy similar to CORM-2 but higher than CORM-3, which presents MICs above 400 μM , but similar to CORM-2 (Table 4.1).

JM94 was not effective against *E. coli* and *S. enterica*. For *E. coli* and *S. enterica*, JM94 was less effective than CORM-2 and CORM-3 (Table 3.4). Additionally, after 4 hours of exposure, JM94 was as toxic as its ligand, clotrimazole. On the contrary, it was bactericidal against *S. aureus* causing a bacterial survival decline to 14 % after 4 hours of exposure to 250 μM , and was as toxic as CORM-2 and more toxic than CORM-3.

Finally, JM106 was not toxic to *E. coli*, *S. enterica* nor *S. aureus* at 250 μM , therefore this CORM is less toxic than CORM-2.

In this work, the only ruthenium-centred CORM that contains an antibiotic molecule is JM94. It is expected that this CORM should be bactericidal towards *S. aureus*, as the antibiotic coordinated to the metal is clotrimazole that by itself is toxic to this bacterium. However, we observed in Gram-negative bacteria, that the ligands 2,2'-bipyridyl and 1,10-phenanthroline are more active than clotrimazole alone. This explains why JM14 and JM16, which contain 2,2'-bipyridyl and 1,10-phenanthroline respectively, are more bactericidal than JM94.

Lastly, JM106 is also a ruthenium centred CORM with 2,2'-bipyridyl as a ligand, but it contains 2 CO groups whereas JM14 contains 3. Of note that the CO load is considered to be important for the bactericidal activity of CORMs, as it is directly related to the amount of CO that is delivered intracellularly. For example, when CORM-3 is dissolved, 1 of its 3 CO groups is lost, meaning that for biological purposes this CORM only has 2 CO molecules. As for, JM14 and JM16 they have a third CO group that is protected by a methoxy group from the water-gas shift reaction^d, a reaction that also occurs when using CORM-3. For this reason, it is possible that JM14 and JM16 may be able to regenerate the third CO group *in vivo*, or that a new group is formed that confers to CORM more toxicity than CORM-3. Therefore, it is reasonable to believe that the methoxy group contributes to the higher toxicity of JM14 and JM16.

Besides JM94, other compounds that combine CORMs with bioactive molecules were studied to test whether their antimicrobial activity would be improved. Among the several manganese CORMs that were tested (Table 3.1), JM46 stands out as the more bactericidal one. JM46 impaired the growth of *E. coli* when used at 35 μM (Figure 3.1). This phenomenon was also visible for *S. enterica*, this bacterium was slightly more resistant to JM46 than *E. coli*, as the survival rates following 2 hours of incubation with JM46 were 73 % and 59 %, respectively (Table 3.3).

^d The water-gas shift reaction is the interaction of a H_2O molecule with a CO molecule to form another species, or to form CO_2 and H_2 . This reaction occurs to one of the CO groups when CORM-3 is dissolved in water⁸³.

Furthermore, JM46 has a MIC of 2.5 μM (2 $\mu\text{g/ml}$) for *S. aureus*, and this CORM reduces the survival to 21 % after only 1 hour of incubation with 10 μM , which indicates that has a quick effect (Table S3). Interestingly, JM46 is more toxic than CORM-2 which presents bactericidal activity against *E. coli* and *S. aureus* of 250 μM , and more toxic than CORM-3 that has bactericidal activities of 400 and 500 μM , respectively (Table 4.1). Moreover, JM46 is more toxic to *E. coli* and *S. aureus* than the manganese CORM ALF 021 which presents a bactericidal activity of 500 μM and 600 μM , respectively (Table 4.1)⁴⁶.

The MICs of JM46 and JM47 against *S. aureus* are 2 and 1 $\mu\text{g/ml}$, respectively, which is in the same order of magnitude as several antibiotics currently in use. For example, for *S. aureus*, the widely used antibiotics amoxicillin and vancomycin have MICs in the range of 0.03 to 128 $\mu\text{g/ml}$ and of 0.06 to 32 $\mu\text{g/ml}$, respectively, depending on the strain⁶⁸.

Altogether these results show that clotrimazole conjugated with CORMs also augments their bactericidal action.

In agreement with our results, other groups also reported the benefits of combining antibiotic or antiparasitic drugs with CORMs as they kill pathogens more efficiently. Pena *et al.* showed that the administration of ALF492 together with artesunate, an antimalarial drug, improves malaria infected-mice survival by 71 %, in comparison with artesunate alone⁶⁹. Murray *et al.* reported that the biofilm production of *P. aeruginosa* is reduced after administration of CORM-2 combined with tobramycin, which is an antibiotic commonly used for lung infections⁷⁰. Furthermore, CORM-2 used in combination with metronidazole strongly decreases *H. pylori* survival⁵².

Rhenium, the transition metal in group 7 of the periodic table, has minimal toxicity towards humans⁷⁴. In this work, rhenium-centred CORMs were analysed. Of these, JM47 seems to be the most toxic of all the compounds tested, since a concentration of 35 μM caused a significant bacteriostatic effect on Gram-negative bacteria (Figures 3.1 and 3.2) and a concentration of 1 μM was bactericidal against *S. aureus*. The survival of *S. aureus* dropped to 24 % after incubation with JM47 (10 μM , for 1 hour), a survival rate that is similar to that observed when using JM46 (Table S3). Interestingly, the incubation of JM47 (35 μM , 1 hour) decreased the survival of *E. coli* to 62 % and of *S. enterica* to 81 % (Tables S1 and S2). *E. coli* cells exposed to JM47 for 3 hours presented a survival rate of 35 % whereas *E. coli* cells exposed to JM46 presented a survival rate of 78 %. Furthermore, JM47 is 500 times more active against *S. aureus* than the water-soluble CORM-3, and 250 times more active than CORM-2. Similarly, JM46 is 200 times more active against *S. aureus* than CORM-3, and 100 times more active than CORM-2. Other rhenium based antibiotic have also been studied. Kumar *et al.* reported that a family of rhenium tricarbonyl triazole complexes were active against *S. aureus*, but not to *E. coli*, and have MICs higher than 16 $\mu\text{g/ml}$ ⁷⁵.

There are several manganese-centred CORMs documented, in particular the first synthesised CORM, i.e., CORM-1. This CORM requires photoactivation in order to release CO, and several variations of this first photoCORM have been prepared, namely $[\text{Mn}(\text{CO})_3(\text{tpa}-\kappa^3\text{N})]\text{Br}$ ⁴⁴. In the

dark, this CORM is non-toxic to *E. coli* even though it is incorporated by the cells. After light irradiation, the bacterial growth is impaired, however, by the same extent as that observed by treatment with CO gas⁷¹. Additionally, CORM-1 was also used to construct a non-woven, that reduced the viability of *S. aureus* within biofilms by 68 % upon irradiation at 405 nm, for 135 minutes⁷². More recently, another manganese photoCORM was produced - EBOR-CORM-1, which is effective against planktonic and biofilm cells of *P. aeruginosa*, but not against *P. aeruginosa* cystic fibrosis lung isolates⁷³. Our group has also studied the bactericidal activity of a manganese CORM, ALF 021, that has antimicrobial activity against both *E. coli* and *S. aureus* (Table 4.1)⁴⁶. Our newly synthesised CORM, JM46, is significantly more active than the manganese centred ALF021 for both *E. coli* and *S. aureus*.

Lecina *et al.* synthesised rhenium complexes containing the antibiotic ciprofloxacin to obtain more efficient antibiotics. However, the two complexes that were carried to antimicrobial studies, named complex 2 and 3, presented similar and lower activity as the free antibiotic, ciprofloxacin, respectively⁷⁶. New rhenium tricarbonyl complexes have also been studied against parasites like *Trypanosoma cruzi*, a protozoan that causes the Chagas disease. The rhenium complexes are 8 to 15 times more active than Nifurtimox, the usually used trypanocidal drug ⁷⁷.

In this work, the toxicity of CORMs to mammalian cells was also tested. The LLC-PK1 mammalian cells that were exposed to JM97, JM107 and JM109 showed IC₅₀ higher than 32 µg/ml and a recovery in cellular viability to 100 % after 72 hours of incubation. The most promising compound, JM109, the ligand of JM107, with MICs of 4 µg/ml to *S. enterica* and 8 µg/ml to *S. aureus* (Table 3.2), has a range of bactericidal action that is significantly lower than the range of toxicity towards mammalian cells. Even though the ligand JM108, is more bactericidal than JM97, it is also more toxic towards mammalian cells. JM108 presents an average IC₅₀ of 26 µg/ml whereas JM97 presents an IC₅₀ higher than 32 µg/ml.

When in comparison with other CORMs, JM46 and JM47 show the highest toxicity against the mammalian cells used, LLC-PK1. Furthermore, the toxicity of these compounds throughout time did not change. Since JM46 and JM47 are structurally similar and only differ in the metal centre, these results indicate that changing the metal centre from manganese to rhenium modified the antimicrobial activity but the cytotoxicity towards mammalian cells remained unaltered.

Among the compounds tested onto mammalian cells, JM46 and JM47 that have a clotrimazole molecule bound are more toxic than clotrimazole alone. Therefore, the toxicity of clotrimazole towards animal cells has increased when this compound is coordinated to the CORM. The manganese complex JM60 is the fourth more toxic compound tested, with IC₅₀ higher than 20 µg/ml, being apparently more toxic to mammalian cells than to bacteria.

Motterlini *et al.* first used myoglobin to measure the CO released from CORMs to the environment, being nowadays the preferred detection method to use the same methodology that was used here to measure the CO liberated from CORMs, as the amount of CO released is related to the toxicity⁴⁴.

We verified that JM46 liberates 3 times more CO than JM47 (Table 3.4). This is probably due to the different nature of the metal centre, since JM46 is a manganese centred CORM and JM47 is a rhenium containing CORM. Furthermore, the difference in the spontaneous liberation of CO groups by each CORM may explain their differences in toxicity towards bacteria, as CORMs that release CO too quickly to the culture media are less efficient, as is the case of JM46. In fact, it has been shown that neither a CO saturated solution nor CORMs devoid of CO are sufficient to impair the growth of bacteria^{42,78}. Hence, we concluded that JM47 is more toxic than JM46 because it is a slower CO releaser.

Microscope images of bacteria incubated with JM46 and JM47 and COP-1 were used to analyse the presence of CO inside bacteria (Figure 3.15). The results showed that JM46 and JM47 enter the bacterial membranes of both Gram-negative and Gram-positive bacteria. However, the CO liberated from JM46 and JM47 into the Gram-negative bacteria *E. coli* and *S. enterica*, as detected by COP-1, does not accumulate homogeneously intracellularly (Figure 3.15).

Bacteria present similar COP-1 fluorescence when incubated with JM46 and JM47, which agrees with the myoglobin assay data that showed that they release similar amounts of CO to the culture medium during the first 30 minutes of reaction. Additionally, JM46 and JM47 are equally toxic during the first 3 hours of incubation with Gram-negative bacteria (Tables S1 and S2). However, the growth curves of the two Gram-negative bacteria exposed to JM47 revealed that the toxic effects remain up to the end of the experiment, indicating that this CORM has a higher time of action than JM46. Once again, this may result from the different release rates of CO of these two CORMs, as JM47 releases CO more gradually than JM46, leading to more long-lasting effects.

Short time incubation with JM46 and JM47 led to an increase in membrane permeability and changes in morphology of approximately half of *E. coli* and *S. enterica* population. For JM46, it was observed that after 24 hours, although the proportion of live and dead cells remained equal, the changes in morphology were no longer observed. However, the proportion of live and dead cells as well as the morphology remains altered when cells were treated with JM47 upon 24 hours. Moreover, albeit the two CORMs affected the membrane permeability, the population of *E. coli* and *S. enterica* was not similarly affected as some bacteria were stained red, orange, yellow and others green. Since all cells come from a single colony, these cells are genetically similar, therefore they are expected to have similar membrane at structural or biochemical levels. Hence, the colour staining differences observed are not associated with the cells themselves but may be due to different cell-CORM interactions.

When *S. aureus* was exposed to JM46 and JM47, the percentage of dead cells is the highest of the three species, which is coherent with a higher sensibility of these bacteria to these specific CORMs. There are no observable morphological changes in *S. aureus*, however, since the MICs for JM46 and JM47 are 2.5 μM and 1 μM , it is not possible to exclude the fact that the concentrations maybe excessively high to detect side effects before the death occurs. Particularly striking were the morphological alterations observed upon exposure to JM46 and JM47 were more evident for *E. coli*, as only after 2 hours cells become elongated and with an apparent doubled in size.

Altogether, treatment with JM46 and JM47 caused alteration in the morphology of cells but to a different extent and homogeneity. The observed heterogeneity upon cellular uptake of the CORMs may result from alteration in the bacterial membrane potential, which controls cell division. In fact, it has been demonstrated that the differences in membrane potential are related with the different quantities of drug uptake by the bacterial cell and the different toxicities⁸⁰. Additionally, pathogenic bacteria are known to change their morphology in order to adapt to multiple environmental conditions to overcome threats to their survival⁸¹. For example, when presented to phagocytes, UPEC start to elongate in order to impair phagocytosis, and this also happens after exposure to β -lactam antibiotics⁸¹. Moreover, the antibiotic nisin causes an acceleration in *Bacillus subtilis* cell division with consequent morphological abnormalities⁸².

5 Conclusions and future perspectives

In this work, in order to better understand the mechanisms that confer CORMs bactericidal properties several newly synthesised compounds were tested in *E. coli*, *S. enterica* and *S. aureus*. Overall, *E. coli* was the most resistant bacterium to CORMs whereas *S. aureus* was the most sensitive one. It was shown that when CORMs are conjugated to bioactive molecules the bactericidal action is enhanced. For example, when clotrimazole was linked to the molecular structure of JM20 and JM20R to form JM46 and JM47, respectively, the bactericidal activity augmented. Of all CORMs tested, JM46 and JM47 are the most active CORMs, and for *S. aureus* JM47 was two times more toxic than JM46. These two CORMs were also toxic to *E. coli* and *S. enterica*, but to a lower extent. JM46 has a different metal-centre than JM47 and is a faster CO releaser, and this has resulted in a lower toxicity. Furthermore, because we have tested several CORMs containing ruthenium, the same metal centre as CORM-3, we could show that the different ligands coordinated to a metal centre also modulate the toxic effect. For example, ruthenium centred JM14 and JM16 that have as ligand 2,2'-bipyridyl and 1,10-phenanthroline, respectively, are more bactericidal than CORM-2 and CORM-3 for *E. coli*, *S. enterica* and *S. aureus*. The JM94, that contains clotrimazole, is more bactericidal than CORM-2 and CORM-3 to *S. aureus*. Finally, the Live and Dead and COP-1 studies revealed that JM46 and JM47 liberate CO intracellularly and increase membrane permeability in *E. coli*, *S. enterica* and *S. aureus*, and induce morphological changes in Gram-negative bacteria.

Altogether these results show that several factors in the chemistry of the CORM modulate its activity towards bacteria, and that the number of CO groups, together with the metal, the ligands and the rate of CO release determine the CORMs toxicity.

The mechanism that underlies the bactericidal properties of CORMs is still widely discussed. This work has contributed to uncover how the chemical composition of the CORMs controls the bactericidal activity. Furthermore, insights into how the CORMs are uptaken by bacterial cells are provided. Future work should include the evaluation of these CORMs to treat infected mammalian cells, i.e. *in vivo* studies. It would also be of interest to test these CORMs onto epithelial cells in order to assess their ability to be used as a topical antimicrobial agent, and onto healthy and cancerous cell lines in order to evaluate if they have antitumoral properties. Altogether, the results contribute to the future synthesis of improved CORM derivatives that are more efficient as bactericidal but less toxic to mammalian cells.

Bibliography

1. Furst, A. Hormetic effects in pharmacology: pharmacological inversions as prototypes for hormesis. *Health Phys.* 52, 527–30 (1987).
2. Braubach, M. et al. Mortality associated with exposure to carbon monoxide in WHO European Member States. *Indoor Air* 23, 115–125 (2013).
3. Romão, C. C., Blättler, W. A., Seixas, J. D. & Bernardes, G. J. L. Developing drug molecules for therapy with carbon monoxide. *Chem. Soc. Rev.* 41, 3571–3583 (2012).
4. Tyrrell, R. Redox regulation and oxidant activation of heme oxygenase-1. *Free Radic. Res.* 31, 335–340 (1999).
5. McCoubrey, W. K., Huang, T. J. & Maines, M. D. Isolation and characterization of a cDNA from the rat brain that encodes hemoprotein heme oxygenase-3. *Eur. J. Biochem.* 247, 725–732 (1997).
6. Morse, D. & Choi, A. M. K. Heme oxygenase-1: the “emerging molecule” has arrived. *Am. J. Respir. Cell Mol. Biol.* 27, 8–16 (2002).
7. Omaye, S. T. Metabolic modulation of carbon monoxide toxicity. *Toxicology* 180, 139–150 (2002).
8. Blumenthal, I. Carbon monoxide poisoning. *J. R. Soc. Med.* 94, 270–272 (2001).
9. Marks, G. S., Brien, J. F., Nakatsu, K. & McLaughlin, B. E. Does carbon monoxide have a physiological function? *Trends Pharmacol. Sci.* 12, 185–188 (1991).
10. Utz, J. & Ullrich, V. Carbon monoxide relaxes ileal smooth muscle through activation of guanylate cyclase. *Biochem. Pharmacol.* 41, 1195–1201 (1991).
11. Carratù, M. R., Renna, G., Giustino, A., De Salvia, M. A. & Cuomo, V. Changes in peripheral nervous system activity produced in rats by prenatal exposure to carbon monoxide. *Arch. Toxicol.* 67, 297–301 (1993).
12. Linden, D. J., Narasimhan, K. & Gurfel, D. Protoporphyrins modulate voltage-gated Ca current in AtT-20 pituitary cells. *J. Neurophysiol.* 70, 2673–2677 (1993).
13. Brouard, S. et al. Carbon monoxide generated by heme oxygenase 1 suppresses endothelial cell apoptosis. *J. Exp. Med.* 192, 1015–1026 (2000).
14. Brooks, J. C. et al. Spoilage and safety characteristics of ground beef packaged in traditional and modified atmosphere packages. *J. Food Prot.* 71, 293–301 (2008).
15. Wegiel, B. et al. Macrophages sense and kill bacteria through carbon monoxide-dependent inflammasome activation. *J. Clin. Invest.* 124, 4926–40 (2014).
16. Nakahira, K. & Choi, A. M. K. Carbon monoxide in the treatment of sepsis. *Am. J. Physiol. - Lung Cell. Mol. Physiol.* 309, L1387–L1393 (2015).
17. Fujita, T. et al. Paradoxical rescue from ischemic lung injury by inhaled carbon monoxide driven by derepression of fibrinolysis. *Nat. Med.* 7, 598–604 (2001).
18. Nakao, A. et al. Carbon monoxide inhalation protects rat intestinal grafts from ischemia/reperfusion injury. *Am. J. Pathol.* 163, 1587–1598 (2003).
19. Fujimoto, H. et al. Carbon monoxide protects against cardiac ischemia-reperfusion injury in vivo via MAPK and Akt-eNOS pathways. *Arterioscler. Thromb. Vasc. Biol.* 24, 1848–1853 (2004).
20. Wu, N. & Veillette, A. SLAM family receptors in normal immunity and immune pathologies. *Curr. Opin. Immunol.* 38, 45–51 (2016).
21. Lee, S. et al. Carbon Monoxide Confers Protection in Sepsis by Enhancing Beclin 1-

- Dependent Autophagy and Phagocytosis. *Antioxid. Redox Signal.* 20, 432–442 (2014).
22. Scharf, D. Scanning Electron Microscope Photography, Video, Motion Pictures, Stock Images, Fine-Art Prints and R&D by David Scharf. Available at: <http://www.scharfphoto.com/>. (Accessed: 2nd February 2018)
 23. Escherich, T. H. The intestinal bacteria of the neonate and breast-fed infant. *Rev. Infect. Dis.* 11, 352–356 (1989).
 24. Blattner, F. R. et al. The complete genome sequence of *Escherichia coli* K-12. *Science* 277, 1453–62 (1997).
 25. Ramotar, K., Conly, J. M. & Louie, T. J. Production of menaquinones by intestinal anaerobes. *J. Infect. Dis.* 150, 213–218 (1984).
 26. Allocati, N., Masulli, M., Alexeyev, M. F. & Di Ilio, C. *Escherichia coli* in Europe: an overview. *Int. J. Environ. Res. Public Health* 10, 6235–54 (2013).
 27. Tornimbene, B. et al. WHO Global Antimicrobial Resistance Surveillance System early implementation 2016-17. *The Lancet Infectious Diseases* (2018). doi:10.1016/S1473-3099(18)30060-4
 28. Russo, T. A. & Johnson, J. R. Medical and economic impact of extraintestinal infections due to *Escherichia coli*: Focus on an increasingly important endemic problem. *Microbes Infect.* 5, 449–456 (2003).
 29. Andino, A. & Hanning, I. *Salmonella enterica*: Survival, colonization, and virulence differences among serovars. *Sci. World J.* 2015, 16 (2015).
 30. Winfiel, M. D. & Groisman, E. A. Role of Nonhost Environments in the Lifestyles of *Salmonella* and *E. coli*. *Appl. Environ. Microbiology* 69, 3687–3694 (2003).
 31. Cossio, M. L. T. et al. *Brock Biology of Microorganism. Instrumentos Familiares XXXIII*, (2012).
 32. Haghkhal, M. Study of virulence factors of *Staphylococcus aureus*. (Faculty of Biomedical and Life Sciences, University of Glasgow, 2003).
 33. Chang, V. S., Dhaliwal, D. K., Raju, L. & Kowalski, R. P. Antibiotic Resistance in the Treatment of *Staphylococcus aureus* Keratitis. *Cornea* 34, 698–703 (2015).
 34. CDC. Antibiotic resistance threats in the United States, 2013. *Current* 114 (2013). doi:CS239559-B
 35. Gardete, S. & Tomasz, A. Mechanisms of vancomycin resistance in *Staphylococcus aureus*. *J. Clin. Invest.* 124, 2836–40 (2014).
 36. Guilfoile, P. G. Antibiotic-Resistant Bacteria. *Deadly Disease and Epidemics* (2007). doi:10.1017/CBO9781107415324.004
 37. Van Cutsem, J. & Thienpont, D. Miconazole, a broad-spectrum Antimycotic Agent with Antibacterial Activity. *Chemotherapy* 17, 392–404 (1972).
 38. Nobre, L. S. et al. Binding ofazole antibiotics to *Staphylococcus aureus* flavohemoglobin increases intracellular oxidative stress. *J. Bacteriol.* 192, 1527–1533 (2010).
 39. Motterlini, R., Mann, B. E. & Foresti, R. Therapeutic applications of carbon monoxide-releasing molecules. *Expert Opin. Investig. Drugs* 14, 1305–1318 (2005).
 40. Romanski, S. et al. Acyloxybutadiene iron tricarbonyl complexes as enzyme-triggered CO-releasing molecules (ET-CORMs). *Angew. Chemie - Int. Ed.* 50, 2392–2396 (2011).
 41. Nobre, L. S., Jeremias, H., Romão, C. C. & Saraiva, L. M. Examining the antimicrobial activity and toxicity to animal cells of different types of CO-releasing molecules. *Dalt. Trans.* 45, 1455–1466 (2016).
 42. Davidge, K. S. et al. Carbon monoxide-releasing antibacterial molecules target respiration

- and global transcriptional regulators. *J. Biol. Chem.* 284, 4516–4524 (2009).
43. Xue, J. & Habtezion, A. Carbon monoxide therapy protects from acute pancreatitis via suppression of TLR4 activation. *Gastroenterology* 142, S318 (2012).
 44. Motterlini, R. et al. Carbon Monoxide-Releasing Molecules: Characterization of Biochemical and Vascular Activities. *Circ. Res.* 90, e17e–24 (2002).
 45. Gullotta, F., Di Masi, A. & Ascenzi, P. Carbon monoxide: An unusual drug. *IUBMB Life* 64, 378–386 (2012).
 46. Nobre, L. S., Seixas, J. D., Romão, C. C. & Saraiva, L. M. Antimicrobial action of carbon monoxide-releasing compounds. *Antimicrob. Agents Chemother.* 51, 4303–4307 (2007).
 47. Sahlberg Bang, C., Kruse, R., Johansson, K. & Persson, K. Carbon monoxide releasing molecule-2 (CORM-2) inhibits growth of multidrug-resistant uropathogenic *Escherichia coli* in biofilm and following host cell colonization. *BMC Microbiol.* 16, 1–10 (2016).
 48. Nobre, L. S., Al-Shahrour, F., Dopazo, J. & Saraiva, L. M. Exploring the antimicrobial action of a carbon monoxide-releasing compound through whole-genome transcription profiling of *Escherichia coli*. *Microbiology* 155, 813–824 (2009).
 49. Tavares, A. F. N. et al. Reactive oxygen species mediate bactericidal killing elicited by carbon monoxide-releasing molecules. *J. Biol. Chem.* 286, 26708–26717 (2011).
 50. Tavares, A. F. N., Nobre, L. S. & Saraiva, L. M. A role for reactive oxygen species in the antibacterial properties of carbon monoxide-releasing molecules. *FEMS Microbiol. Lett.* 336, 1–10 (2012).
 51. Desmard, M. et al. A carbon monoxide-releasing molecule (CORM-3) exerts bactericidal activity against *Pseudomonas aeruginosa* and improves survival in an animal model of bacteraemia. *FASEB J.* 23, 1023–1031 (2009).
 52. Tavares, A. F. et al. The bactericidal activity of carbon monoxide-releasing molecules against helicobacter pylori. *PLoS One* 8, (2013).
 53. Simpson, P. V., Nagel, C., Bruhn, H. & Schatzschneider, U. Antibacterial and Antiparasitic Activity of Manganese(I) Tricarbonyl Complexes with Ketoconazole, Miconazole, and Clotrimazole Ligands. *Organometallics* 34, 3809–3815 (2015).
 54. Iwata, K., Yamaguchi, H. & Hiratani, T. Mode of action of clotrimazole. *Sabouraudia J. Med. Vet. Mycol.* 11, 158–166 (1973).
 55. Betanzos-Lara, S. et al. Cytotoxic copper(II), cobalt(II), zinc(II), and nickel(II) coordination compounds of clotrimazole. *J. Inorg. Biochem.* 114, 82–93 (2012).
 56. Tinajero-Trejo, M. et al. Antimicrobial Activity of the Manganese Photoactivated Carbon Monoxide-Releasing Molecule [Mn(CO)₃(tpa-κ³N)]⁺ Against a Pathogenic *Escherichia coli* that Causes Urinary Infections. *Antioxid. Redox Signal.* 24, 765–780 (2016).
 57. Jorgensen, J. H. & Ferraro, M. J. Antimicrobial Susceptibility Testing: A Review of General Principles and Contemporary Practices. *Clin. Infect. Dis.* 49, 1749–1755 (2009).
 58. Cockerill, F. R., Wikler, M. A., Alder, J. & Dudley, M. N. Methods for Dilution Antimicrobial Susceptibility Tests for Bacteria That Grow Aerobically. *Contemp. Clin. Dent.* 32, 88 (2011).
 59. Michel, B. W., Lippert, A. R. & Chang, C. J. A Reaction-Based Fluorescent Probe for Selective Imaging of Carbon Monoxide in Living Cells Using a Palladium-Mediated Carbonylation. *J. Am. Chem. Soc.* 134, 15668–15671 (2012).
 60. Mattson, A., Jensen, C. & Dutcher, R. Triphenyltetrazolium Chloride as a Dye for Vital Tissues. *Science* (80-.). 106, 294–295 (1947).
 61. Mosmann, T. Rapid colorimetric assay for cellular growth and survival: Application to proliferation and cytotoxicity assays. *J. Immunol. Methods* 65, 55–63 (1983).
 62. WHO. Health Care Without Avoidable Infection. The Critical Role of Infection Prevention

- and Control. 16 (2016). Available at: <http://apps.who.int/iris/bitstream/handle/10665/246235/WHO-HIS-SDS-2016.10-eng.pdf?sequence=1>. (Accessed: 2nd August 2018)
63. Herndon, D. N., William Curreri, P., Abston, S., Rutan, T. C. & Barrow, R. E. Treatment of burns. *Curr. Probl. Surg.* 24, 347–397 (1987).
 64. Bassetti, S., Hu, J., D'Agostino, J. & Sherertz, R. J. Prolonged antimicrobial activity of a catheter containing chlorhexidine-silver sulfadiazine extends protection against catheter infections in vivo. *Antimicrob. Agents Chemother.* 45, 1535–1538 (2001).
 65. Li, F., Collins, J. G. & Keene, F. R. Ruthenium complexes as antimicrobial agents. *Chem. Soc. Rev.* 44, 2529–2542 (2015).
 66. Li, F. et al. In vitro susceptibility and cellular uptake for a new class of antimicrobial agents: Dinuclear ruthenium(II) complexes. *J. Antimicrob. Chemother.* 67, 2686–2695 (2012).
 67. Bolhuis, A. et al. Antimicrobial activity of ruthenium-based intercalators. *Eur. J. Pharm. Sci.* 42, 313–317 (2011).
 68. Andrews, J. M. & Andrews, J. M. Determination of minimum inhibitory concentrations. *J. Antimicrob. Chemother.* 48 Suppl 1, 5–16 (2001).
 69. Pena, A. C. et al. A novel carbon monoxide-releasing molecule fully protects mice from severe malaria. *Antimicrob. Agents Chemother.* 56, 1281–1290 (2012).
 70. Murray, T. S. et al. The carbon monoxide releasing molecule CORM-2 attenuates *Pseudomonas aeruginosa* biofilm formation. *PLoS One* 7, 1–11 (2012).
 71. Emsley, J. Rhenium. in *Nature's Building Blocks: An A-Z Guide to the Elements* 358–360 (Oxford University Press, 2003).
 72. Kumar, S. V., Lo, W. K. C., Brooks, H. J. L., Hanton, L. R. & Crowley, J. D. Antimicrobial Properties of Mono- and Di-fac-rhenium Tricarbonyl 2-Pyridyl-1,2,3-triazole Complexes. *Aust. J. Chem.* 69, 489 (2016).
 73. Nagel, C. et al. Introducing $[Mn(CO)_3(tpa-\kappa 3N)]^+$ as a novel photoactivatable CO-releasing molecule with well-defined iCORM intermediates – synthesis, spectroscopy, and antibacterial activity. *Dalt. Trans.* 43, 9986 (2014).
 74. Klinger-Strobel, M. et al. Bactericidal effect of a photoresponsive carbon monoxide releasing non-woven against *Staphylococcus aureus* biofilms. *Antimicrob. Agents Chemother.* 60, 4037–4046 (2016).
 75. Flanagan, L. et al. The antimicrobial activity of a carbon monoxide releasing molecule (EBOR-CORM-1) is shaped by intraspecific variation within *Pseudomonas aeruginosa* populations. *Front. Microbiol.* 9, 1–11 (2018).
 76. Lecina, J., Cortés, P., Llagostera, M., Piera, C. & Suades, J. New rhenium complexes with ciprofloxacin as useful models for understanding the properties of $[^{99m}Tc]$ -ciprofloxacin radiopharmaceutical. *Bioorganic Med. Chem.* 22, 3262–3269 (2014).
 77. Rodríguez Arce, E. et al. Rhenium(I) tricarbonyl compounds of bioactive thiosemicarbazones: Synthesis, characterization and activity against *Trypanosoma cruzi*. *J. Inorg. Biochem.* 170, 125–133 (2017).
 78. Nobre, L. *Unravelling Novel Modes of Antimicrobial Action*. (Universidade Nova de Lisboa, 2010).
 79. Dampert, P. D. & Epstein, W. Role of the membrane potential in bacterial resistance to aminoglycoside Role of the Membrane Potential in Bacterial Resistance to Aminoglycoside Antibiotics. 20, 803–808 (1981).
 80. Justice, S. S., Hunstad, D. A., Cegelski, L. & Hultgren, S. J. Morphological plasticity as a bacterial survival strategy. *Nat. Rev. Microbiol.* 6, 162–168 (2008).

81. Hyde, A. J., Parisot, J., McNichol, A. & Bonev, B. B. Nisin-induced changes in *Bacillus* morphology suggest a paradigm of antibiotic action. *Proc. Natl. Acad. Sci.* 103, 19896–19901 (2006).
82. Motterlini, R. et al. Bioactivity and pharmacological actions of carbon monoxide-releasing molecules. *Curr. Pharm. Des.* 9, 2525–39 (2003).

Supplementary material

Table S1 Percentage of survival of *Escherichia coli* over the course of 24 hours of incubation with 35 μ M of JM46, JM20, JM47, JM20R, clotrimazole and 1 % of DMSO.

CORMs	Survival of <i>E. coli</i> (%)							
	Incubation time							
	1	2	3	4	5	6	7	24
JM46	70 \pm 4	59 \pm 2	78 \pm 7	94 \pm 8	96 \pm 14	91 \pm 7	83 \pm 3	94 \pm 6
JM20	94 \pm 4	90 \pm 6	90 \pm 8	119 \pm 16	93 \pm 20	107 \pm 5	83 \pm 5	95 \pm 5
JM47	62 \pm 8	46 \pm 9	35 \pm 10	28 \pm 11	25 \pm 6	21 \pm 8	14 \pm 2	25 \pm 5
JM20R	95 \pm 4	92 \pm 6	99 \pm 8	104 \pm 9	106 \pm 18	116 \pm 10	86 \pm 15	110 \pm 8
Clotrimazole	91 \pm 9	74 \pm 21	109 \pm 9	119 \pm 7	98 \pm 17	114 \pm 14	92 \pm 6	101 \pm 13
DMSO	95 \pm 4	93 \pm 7	102 \pm 4	109 \pm 11	98 \pm 11	111 \pm 10	88 \pm 14	101 \pm 7

Table S2 Percentage of survival of *Salmonella enterica* over the course of 24 hours of incubation with 35 μ M of JM46, JM20, JM47, JM20R, clotrimazole and 1 % of DMSO.

CORMs	Survival of <i>S. enterica</i> (%)							
	Incubation time (hours)							
	1	2	3	4	5	6	7	24
JM46	84 \pm 8	73 \pm 12	92 \pm 24	105 \pm 6	107 \pm 27	109 \pm 22	115 \pm 16	134 \pm 16
JM20	100 \pm 0	97 \pm 1	119 \pm 30	110 \pm 10	121 \pm 26	98 \pm 3	104 \pm 11	111 \pm 18
JM47	81 \pm 2	62 \pm 8	60 \pm 6	63 \pm 2	52 \pm 21	46 \pm 7	47 \pm 9	39 \pm 9
JM20R	100 \pm 1	94 \pm 6	98 \pm 4	105 \pm 11	117 \pm 29	101 \pm 9	111 \pm 9	100 \pm 8
Clotrimazole	100 \pm 1	98 \pm 2	102 \pm 16	101 \pm 7	102 \pm 9	95 \pm 13	98 \pm 7	126 \pm 36
DMSO	98 \pm 2	97 \pm 5	95 \pm 17	100 \pm 9	106 \pm 25	88 \pm 4	103 \pm 9	117 \pm 22

Table S3 Percentage of survival of *Staphylococcus aureus* over the course of 24 hours of incubation with 10 μ M of JM46, JM20, JM47, JM20R, clotrimazole and 1 % of DMSO.

CORMs	Survival of <i>S. aureus</i> (%)							
	Incubation time (hours)							
	1	2	3	4	5	6	7	24
JM46	21 \pm 3	8 \pm 1	4 \pm 1	2 \pm 1	2 \pm 0	1 \pm 0	1 \pm 0	1 \pm 6
JM20	97 \pm 2	99 \pm 6	97 \pm 10	96 \pm 10	107 \pm 15	85 \pm 10	95 \pm 26	95 \pm 4
JM47	24 \pm 4	9 \pm 1	4 \pm 1	3 \pm 1	2 \pm 0	2 \pm 0	2 \pm 0	1 \pm 9
JM20R	94 \pm 5	98 \pm 10	79 \pm 18	92 \pm 14	100 \pm 14	83 \pm 5	113 \pm 23	94 \pm 14
Clotrimazole	68 \pm 8	54 \pm 3	47 \pm 5	40 \pm 10	48 \pm 3	50 \pm 3	63 \pm 14	47 \pm 7
DMSO	97 \pm 1	98 \pm 4	93 \pm 6	91 \pm 13	89 \pm 7	82 \pm 1	97 \pm 18	95 \pm 2